CENTER FOR ASTROPHYSICS
HARVARD & SMITHSONIAN

ASIAA

Submillimeter Array Newsletter

Number 33, January 2022

CONTENTS

FROM THE DIRECTOR

Dear SMA Newsletter readers,

The SMA continued to conduct high-quality science observations throughout 2021, though with reduced throughput as a result of evolving pandemic restrictions imposed on staff members in order to maintain a safe and healthy work environment. Here, I invite you join me in thanking SMA staff members for their continued commitment and dedication to the observatory. In particular I thank those who have, on a daily basis, provided on-site technical support on Maunakea, and those in Cambridge who have continued to support observations by maintaining, repairing, and upgrading instrumentation as needed. We are grateful to our telescope operators in Hilo, Cambridge, and Taipei for their continued commitment to the observatory. Less visible, but also deserving of our thanks are SMA staff, fellows, and students still working at home, who continue to support SMA science and operations.

To help maintain the robustness of the array during this difficult period, the SMA will be pausing scientific operations during the month of February in order to facilitate major engineering and maintenance work, some of which had been deferred or otherwise impacted by the pandemic. This will include major improvements to the backbone infrastructure of the real-time software monitor and control systems, as well as preventive maintenance to help keep the array running at full capability. We look forward to being able to provide our users with a more robust SMA in the months and years to follow, including during the upcoming 2022A semester, for which a call for proposals will be released shortly.

We begin the new year with exciting times ahead. The third SMA Interferometry School starts on January 18th. The installation of the first set of zero-IF receivers, which will enable the SMA to provide contiguous spectral line coverage of more than 32 GHz with each receiver, will be completed in the coming months, followed by on-sky verification of performance. Finally, the first of the prototype wSMA receiver systems will be installed in an SMA antenna later this year, with first light to follow shortly thereafter.

As we enter this exciting period of developments at the SMA, we thank you for your continued support. May this year be kind to you all!

Best wishes,

Raymond Blundell

MASSIVE MOLECULAR GAS RESERVOIR IN A LUMINOUS SUB-MILLIMETER GALAXY DURING COSMIC NOON

Bin Liu, N. Chartab, H. Nayyeri, A. Cooray, C. Yang, D.A Riechers, M. Gurwell, Zong-hong Zhu, S. Serjeant, E. Borsato, L. Marchetti, M. Negrello, E.M. Corsini, and P. van der Werf

Through *Herschel* wide-area surveys, we have now identified hundreds of extremely bright sub-millimeter sources ($s_{500\mu m} \geq 100$ mJy) at high redshifts. We have selected a very bright Keck/NIRC2 observed Einstein ring lensed sub-millimeter galaxy (SMG) at z = 2.553 (HERS J020941.1+001557 designated as HERS1 hereafter.). This target is identified from the *Herschel* Stripe 82 survey (Viero et al. 2014) covering 81 deg^2 with *Herschel*/SPIRE instrument at 250, 350, and 500μm and

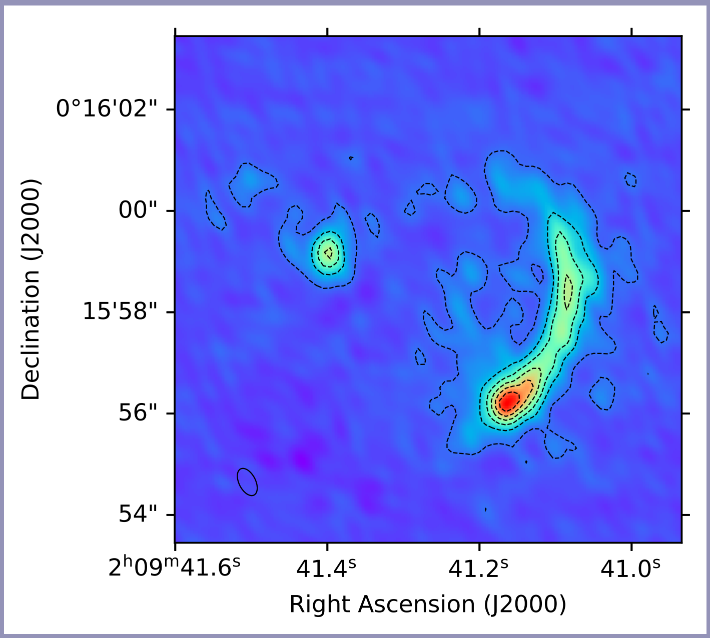

Figure 1: The high-resolution SMA 870 μm continuum map combining SUB+EXT+VEX configurations. The final image peaks over 17mJy beam^{-1} and has an rms of 305 μJy beam^{-1}. Black dash lines show the contours starting from -6σ and increase in steps of 9σ.

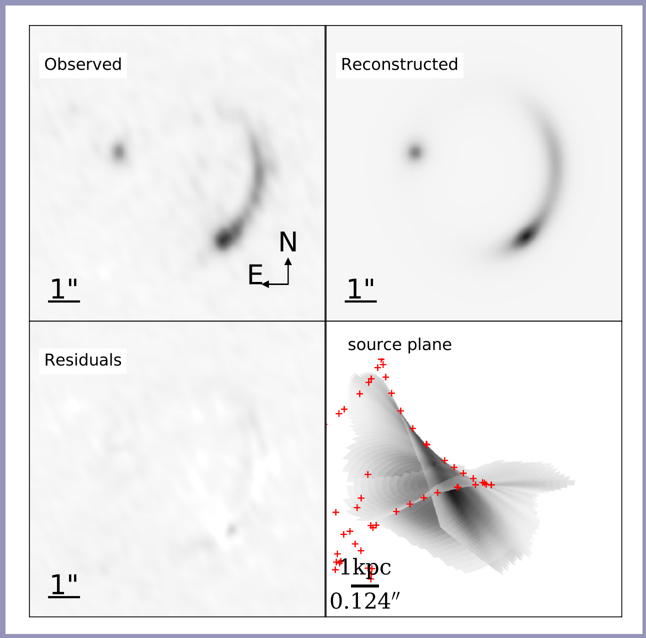

Figure 2: The SMA 870 μm continuum image along with modelling results using the best-fit model derived from the high resolution HST image. Red cross symbols represent the caustic line.

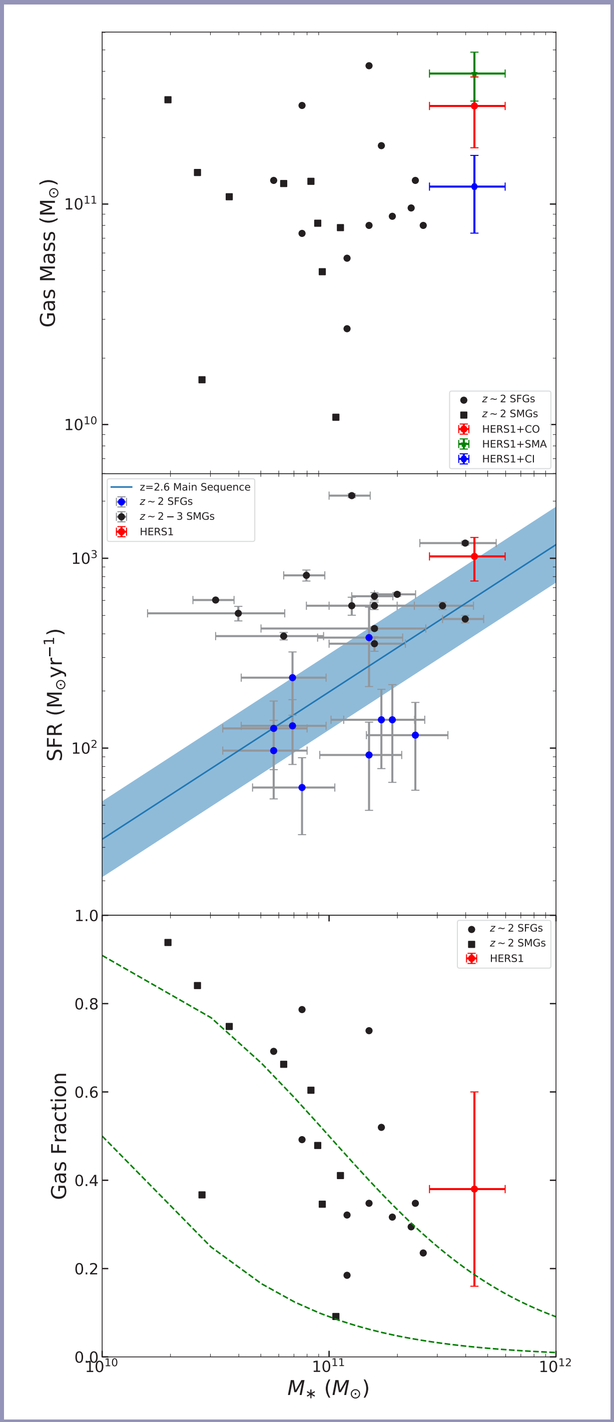

Figure 3: Top: molecular gas mass calculated from the CO (1-0) line (red), CI line (blue) and the SMA 870 µm continuum data (green) along with SFGs and SMGs at similar redshifts. **Middle:** stellar mass vs. star formation rate of HERS1. The blue line and shadow blue area show the z = 2.6 trend and a 0.2 dex scatter. SFGs at z ~ 2 and SMGs at at z ~ 2–3 are presented for comparison. **Bottom:** similar with the top panel but shows molecular gas fraction. The fraction of HERS1 takes the average value of three HERS1 data. The green dash lines represent a constant stellar mass of 10^{10} $M_\odot$ and 10^{11} $M_\odot$, respectively.

was first identified as a gravitationally lensed radio source by two foreground galaxies at z = 0.202 in a citizen science project (Geach et al. 2015) to an Einstein-ring with a radius ~3''. HERS1 has extensive follow-up observations including a sub-millimeter observation by SMA at 870µm. The wealth of multi-band data combined with high resolution deep imaging provide a unique opportunity to study physical properties of HERS1 as an extremely bright sub-millimeter galaxy during the peak epoch of star formation activity.

SMA observations of HERS1 were performed at three different times and in three separate array configurations. By combining these three configurations, we obtained the highest resolution SMA image as shown in Figure 1. Using natural weighting of the visibilities, the synthesized resolution is 580 mas × 325 mas (PA 27.2 deg), and the achieved rms in the combined data map is 305 µJy beam^{-1}. The final map shows a detailed partial Einstein ring with a radius of 3''. Using the best-fit model built from the high-resolution HST/WFC3 F125W image, we can reconstruct the lens and source plane images, the results are illustrated in Figure 2. From this we obtain the luminosity-weighted magnification factor of dust emission μ_{dust} = 12.8 ± 0.3 which is similar to the stellar factor μ_{star} = 13.6 ± 0.4.

The observed flux of SMA continuum is 160 ± 3 mJy. We corrected the observed multi-band flux densities by magnification derived from the HST and SMA map and performed an SED fitting. Combing all the photometry results, the best-fit model gives a total intrinsic infrared luminosity of L_{IR}=(1.0±0.3)×$10^{13}L_\odot$, which makes it one of the hyper-luminous galaxies at high-redshifts. The corresponding star formation rate (SFR) is 1023±264$M_\odot$yr^{-1} assuming a Chabrier initial mass function (Chabrier 2003). HERS1 also possesses a large value of stellar mass of $4.4^{+2.2}_{-1.0}$×$10^{11}M_\odot$. This is in agreement with simulations (Dav´e et al. 2010) and model requirements of sub-millimeter bright galaxies (Hayward et al. 2011). The stellar mass and SFR relation is shown in the top panel of Figure 3. For the dust temperature, the best-fit result is T_d=$35.1^{+1.9}_{-1.4}$K.

The molecular gas mass derived from the SMA data is (4.49±1.12)×$10^{11}M_\odot$. Using the star-formation rate, and the average gas mass measured from the SMA, CO and CI, we can derive the gas depletion timescale t_{dep}≡M_{gas}/SFR. HERS1 has a gas depletion of ~257 Myr, this is much smaller than the star-forming galaxies ~1 Gyr (e.g. Kennicutt 1998; Genzel et al. 2010; Saintonge et al. 2011; Decarli et al. 2016a,b) and a 'main sequence' ~0.7 Gyr or even shorter (Tacconi et al. 2013; Sargent et al. 2014; Saintonge et al. 2013). The gas fraction f_{gas} can be calculated as $M_{gas}/(M_*+ M_{gas})$.

HERS1 has a low gas fraction with f_{gas} = 0.38±0.22 as shown in the top panel of Figure 3, the low gas fraction and high stellar mass indicate that HERS1 has formed most of its stars. The short gas depletion time, compared to 1 Gyr for typical SFGs at z ~ 2, suggests that HERS1 will become quiescent shortly in the lack of cool gas replenishment.

In conclusion, we analyze the physical conditions of a typical sub-millimeter galaxy through multi-band observations including the SMA at 870 μm. Further details of this work have been reported in the paper by Liu et al. (2021).

REFERENCES

- Chabrier, G. 2003, PASP, 115, 763 Dav´e, R., Finlator, K., Oppenheimer, B. D., et al. 2010, Monthly Notices of the Royal Astronomical Society, 404, 1355
- Decarli, R., Walter, F., Aravena, M., et al. 2016a, The Astrophysical Journal, 833, 69 —. 2016b, The Astrophysical Journal, 833, 70
- Geach, J. E., More, A., Verma, A., et al. 2015, MNRAS, 452, 502
- Genzel, R., Tacconi, L. J., Gracia-Carpio, J., et al. 2010, Monthly Notices of the Royal Astronomical Society, 407, 2091
- Hayward, C. C., Kereˇs, D., Jonsson, P., et al. 2011, The Astrophysical Journal, 743, 159
- Kennicutt, Robert C., J. 1998, ApJ, 498, 541
- Liu, B., Chartab, N., Nayyeri, H., et al. 2021, arXiv e-prints, arXiv:2108.13016
- Saintonge, A., Kauffmann, G., Wang, J., et al. 2011, Monthly Notices of the Royal Astronomical Society, 415, 61
- Saintonge, A., Lutz, D., Genzel, R., et al. 2013, ApJ, 778, 2
- Sargent, M. T., Daddi, E., B´ethermin, M., et al. 2014, The Astrophysical Journal, 793, 19
- Tacconi, L. J., Neri, R., Genzel, R., et al. 2013, ApJ, 768, 74
- Viero, M. P., Asboth, V., Roseboom, I. G., et al. 2014, ApJS, 210, 22

DOES THE MAGNETIC FIELD SUPPRESS FRAGMENTATION IN MASSIVE DENSE CORES?

Aina Palau,[1] Qizhou Zhang,[2] Josep Miquel Girart,[3,4] Junhao Liu,[2,5,6] Ramprasad Rao,[2] Patrick M. Koch,[7] Robert Estalella,[8] Huei-Ru Vivien Chen,[9] Hauyu Baobab Liu,[7] Keping Qiu,[5,6] Zhi-Yun Li,[10] Luis A. Zapata,[1] Sylvain Bontemps,[11] Paul T. P. Ho,[7] Henrik Beuther,[12] Tao-Chung Ching,[7] Hiroko Shinnaga,[13] and Aida Ahmadi[14]

Understanding the fragmentation process of molecular clouds is crucial because it is intimately related to the formation of star clusters. Magnetic fields have been proposed as a key ingredient in the fragmentation process of molecular clouds, since a large number of theoretical and numerical works indicate that strong magnetic fields provide a form of support against gravitational contraction (e.g., Boss 2004; Price & Bate 2007; Commerçon et al. 2011; Peters et al. 2011; Myers et al. 2013; Boss & Keiser 2014; Hennebelle & Inutsuka 2019). Therefore, magnetic fields should naturally suppress fragmentation.

Star cluster forming cores are often associated with the so-called massive dense cores, cores with masses of 50-1000 $M_\odot$, and with sizes of 0.1-0.5 pc. It is expected that a massive dense core with weak magnetic fields should highly fragment, giving birth to a rich stellar cluster while, on the other hand, a massive dense core threaded by strong magnetic fields would be less fragmented, giving birth to more isolated high-mass stars. However, the aforementioned theoretical prediction has never been tested observationally in a relatively large (more than 10 objects) sample of cluster forming clouds.

We compiled a sample of 18 massive dense cores for which submillimeter polarization observations from the Legacy Program of the SMA (Zhang et al. 2014), as well as submillimeter continuum images at high angular resolution were available. The sample was built to strictly fulfill constraints of reaching spatial resolutions of ~1000 au and mass sensitivities (from the submillimeter continuum) around ~0.5 $M_\odot$, so that a fragmentation level can be measured in a uniform and reliable way (and within the same field of view of ~0.15 pc) for all the cores. Fig.1 presents the submillimeter continuum emission at 870 μm obtained with the extended configuration of the SMA (or NOEMA for the 1.3 mm emission, Beuther et al. 2018), along with the magnetic field overplotted in blue line segments.

A total number of 160 fragments were identified within the 18 massive dense cores. We assigned a fragmentation level within a field of view of 0.15 pc, N_{mm}, to each massive dense core. We found a variety of fragmentation levels and, additionally, cores were classified according to their fragmentation type, mainly `aligned fragmentation', `clustered fragmentation', and `no fragmentation'.

In order to obtain the magnetic field strength and the mass-to-magnetic flux ratio (mass-to-flux ratio, for short), it is necessary to have estimates of the velocity dispersion of turbulence, the density structure of the core, and the dispersion of polarization position angles (PA) of the perturbed component of the magnetic field. With these data, the Davis-Chandrasekhar-Fermi method (DCF, Davis 1951, Chan-

[1] Instituto de Radioastronomía y Astrofísica, Universidad Nacional Autónoma de México; [2] Center for Astrophysics | Harvard & Smithsonian; [3] Institut de Ciències de l'Espai (CSIC-IEEC); [4] Institut d'Estudis Espacials de Catalunya; [5] School of Astronomy and Space Science, Nanjing University ; [6] Key Laboratory of Modern Astronomy and Astrophysics (Nanjing University), Ministry of Education; [7] Institute of Astronomy and Astrophysics, Academia Sinica; [8] Departament de Física Quántica i Astrofísica, Institut de Ciències del Cosmos, Universitat de Barcelona, (IEEC-UB); [9] Institute of Astronomy and Department of Physics, National Tsing Hua University; [10] Astronomy Department, University of Virginia; [11] Université de Bordeaux, Laboratoire d'Astrophysique de Bordeaux, CNRS/INSU, UMR; [12] Max Planck Institute for Astronomy; [13] Department of Physics and Astronomy, Graduate School of Science and Engineering, Kagoshima University, Amanogawa Galaxy Astronomy Research Center; [14] Leiden Observatory, Leiden University

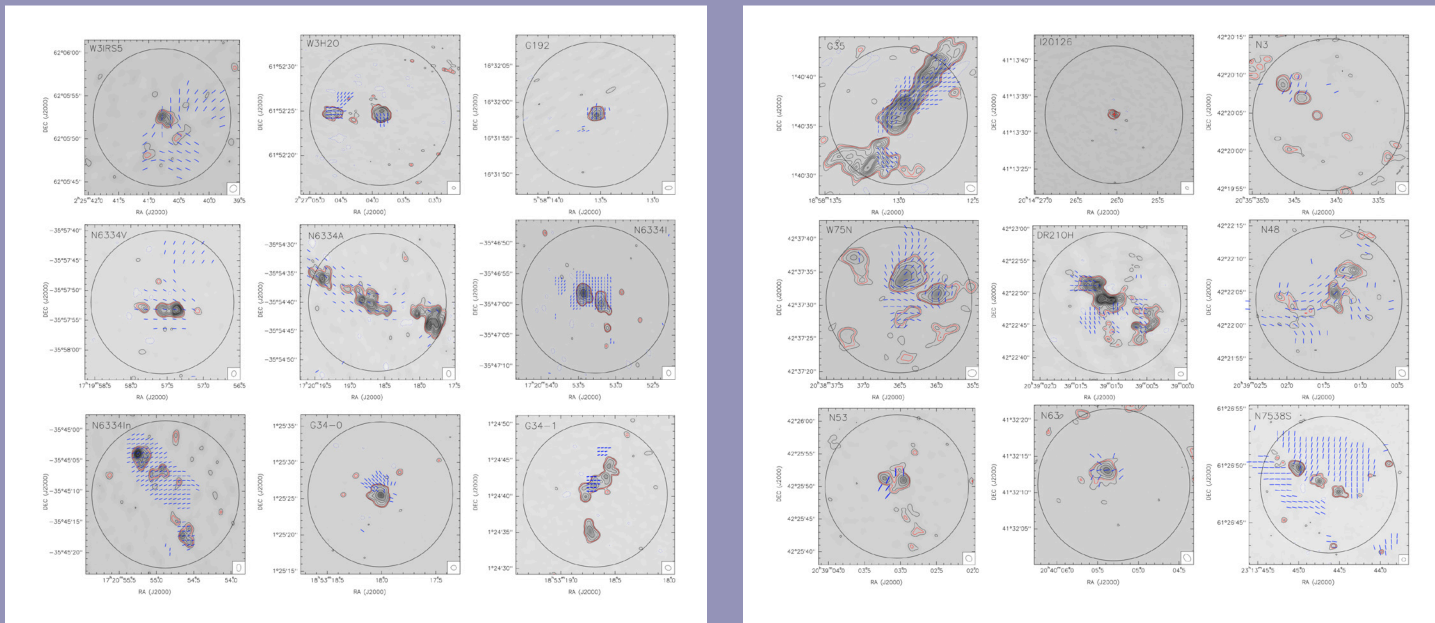

Figure 1: 0.87 or 1.3 mm continuum high-angular-resolution maps with the magnetic field overplotted in blue line segments. First and second black contours correspond to 4 and 8 times the rms noise in each region. The red contour corresponds to the identification level of 6σ. Synthesized beams are plotted in the bottom-right corner of each panel, and the black circle corresponds to the common field of view of 0.15 pc diameter.

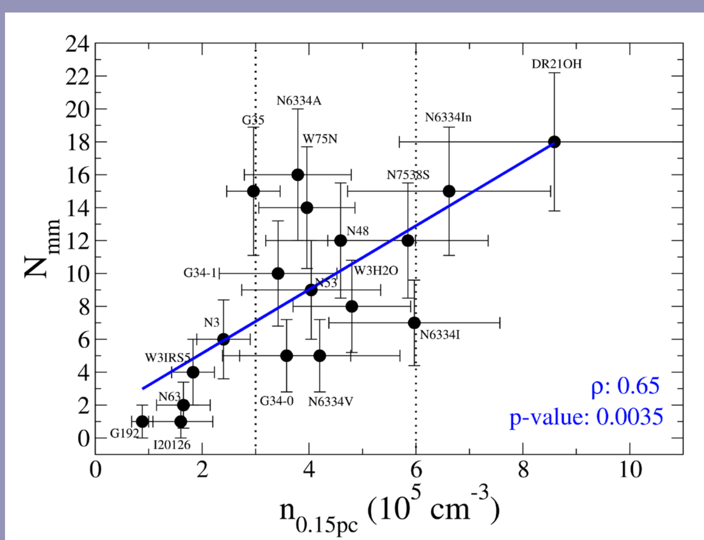

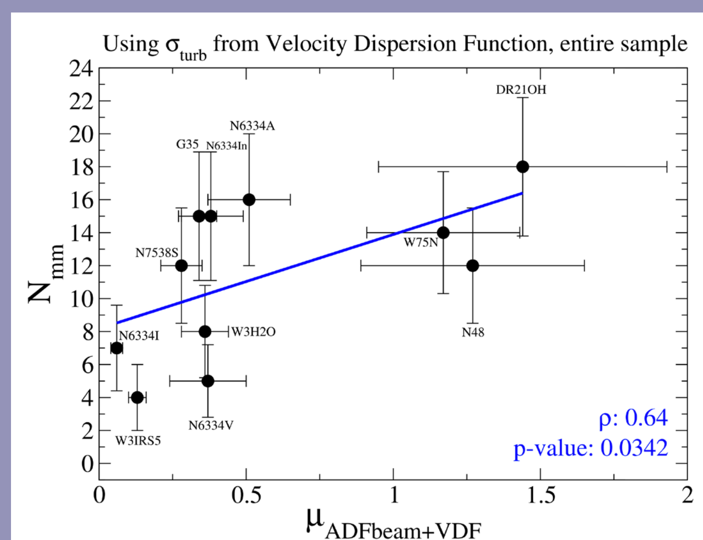

Figure 2: Fragmentation level vs. density averaged within the same field of view where fragmentation, velocity dispersion, and polarization PA dispersion were assessed (0.15 pc in diameter). The blue line indicates the result of a linear regression, with a correlation coefficient of 0.71. The Spearman's rank correlation coefficient rho and the p value are annotated in the bottom-right corner.

Figure 3: Fragmentation level vs. mass-to-flux ratio. The mass-to-flux ratio was inferred using the smallest value (at the beam scale) of the ADF (following Hildebrand et al. 2009) for the polarization PA dispersion and using the smallest value (at the beam scale) of the VDF for the velocity dispersion. This allowed to separate the perturbed magnetic and velocity fields from the ordered large-scale field. The blue line indicates the result of a linear regression, with a correlation coefficient of 0.58. The Spearman's rank correlation coefficient rho and the p value are annotated in the bottom-right corner.

drasekhar & Fermi 1953) can be applied to infer the magnetic field strength and the mass-to-flux ratio.

The $H^{13}CO^+$ (4-3) data from the SMA observations were used to infer velocity dispersions for each core after obtaining an average spectrum of each region. In addition, the velocity dispersion function (VDF) was calculated using the first-order moment image of the $H^{13}CO^+$ (4-3) line for each core. This was done in order to separate the turbulent (small-scale) component of the velocity field from the large-scale component that is more associated with systematic motions (infall/outflow/rotation).

The temperature and density structure were modeled for each massive dense core using submillimeter continuum emission from single-dish telescopes and the spectral energy distribution, following Palau et al. (2014).

Four approaches were used to estimate polarization PA dispersions. First, the PA dispersion was estimated from the standard deviation of the PA corrected for the PA uncertainties. Second, different Gaussians were fitted to the PA histograms. Third, the angular dispersion function (ADF) analysis was performed following Houde et al. (2009), and, fourth, the PA dispersion was estimated from the smallest value (at the beam scale) of the ADF (following Hildebrand et al. 2009). It was found that a robust way to estimate the magnetic field strength seems to be the following: to use, in the DCF calculation, the velocity dispersion at the smallest (beam) scales (obtained from the VDF), and the PA dispersion at the smallest (beam) scales (obtained from the ADF following Hildebrand et al. 2009). This allows to separate, for *both* the velocity field and the polarization PAs, the perturbed or turbulent component from a more ordered large-scale component.

Our main results reveal a strong correlation of N_{mm} with density averaged within 0.15 pc although with a significant scatter (see Fig. 2). In addition, N_{mm} seems to tentatively correlate with the mass-to-flux ratio (see Fig. 3), as expected from the theoretical and numerical works. While these findings need to be investigated further in larger samples with more sensitive observations, this study constitute the first observational evidence that the magnetic field seems to suppress fragmentation. Further details of this work have been published in Palau et al. (2021).

REFERENCES

- Beuther, H., Mottram, J. C., Ahmadi, A., et al. 2018, A&A, 617, A100
- Boss, A. P. 2004, MNRAS, 350, L57
- Boss, A. P., & Keiser, S. A. 2014, ApJ, 794, 44
- Chandrasekhar, S., & Fermi, E. 1953, ApJ, 118, 113
- Commerçon, B., Hennebelle, P., & Henning, T. 2011, ApJL, 742, L9
- Davis, L. 1951, PhRv, 81, 890
- Hennebelle, P., & Inutsuka, S.-. i. 2019, FrASS, 6, 5
- Hildebrand, R. H., Kirby, L., Dotson, J. L., et al. 2009, ApJ, 696, 567
- Houde, M., Vaillancourt, J. E., Hildebrand, R. H., et al. 2009, ApJ, 706, 1504
- Myers, A. T., McKee, C. F., Cunningham, A. J., et al. 2013, ApJ, 766, 97
- Palau, A., Estalella, R., Girart, J. M., et al. 2014, ApJ, 785, 42
- Palau, A., Zhang, Q., Girart, J. M. et al. 2021, ApJ, 912, 159
- Peters, T., Banerjee, R., Klessen, R. S., et al. 2011, ApJ, 729, 72
- Price, D. J., & Bate, M. R. 2007, MNRAS, 377, 77
- Zhang, Q., Qiu, K., Girart, J. M., et al. 2014, ApJ, 792, 116

MULTI-SCALE DUST POLARIZATION AND SPIRAL-LIKE STOKES-I RESIDUAL IN THE CLASS I PROTOSTELLAR SYSTEM TMC-1A

Yusuke Aso[1], Woojin Kwon[2,3], Naomi Hirano[4], Tao-Chung Ching[5,6], Shih-Ping Lai[4,7,8], Zhi-Yun Li[9], and Ramprasad Rao[10]

Recent interferometric observations of polarized emission in molecular clouds have unveiled magnetic fields on envelope scales (100-1000 au) around protostars, enabling us to investigate magnetic effects on star formation. For example, a magnetic field in an hourglass shape implies that the field is dragged by infalling materials (e.g., Maury et al. 2018). A more quantitative verification of this scenario requires kinematic information, such as an infall velocity, as well as the field strength.

TMC-1A (IRAS 04365+2535) is a Class I protostar with a bolometric luminosity of 2.7 $L_\odot$ and a bolometric temperature of 118 K (Kristensen et al. 2012) in the Taurus molecular cloud at a distance of 140 pc (Galli et al. 2018). Previous observational

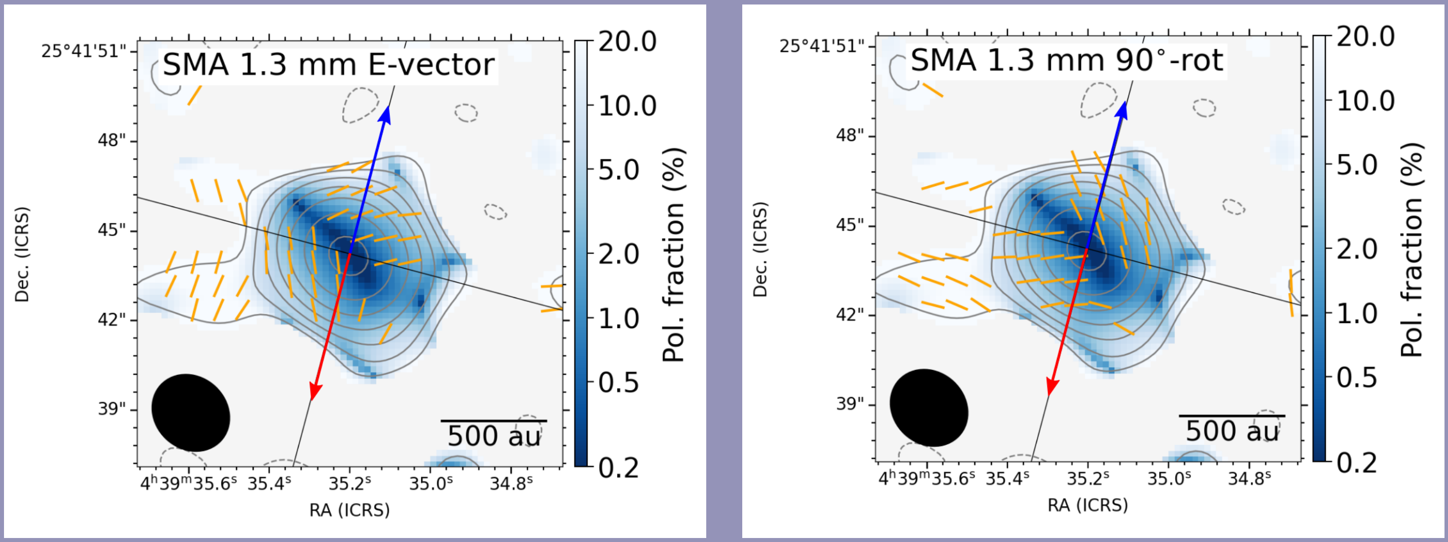

Figure 1: The polarized continuum emission at 1.3 mm (orange line segments and color scales) observed with the SMA. The contours show the Stokes I continuum emission. The diagonal line denotes the major axis (P.A.=75°) of the TMC-1A disk, and the red and blue arrows mark the outflow axis.

[1] Korea Astronomy and Space Science Institute (KASI); [2] Department of Earth Science Education, Seoul National University; [3] SNU Astronomy Research Center, Seoul National University; [4] Academia Sinica Institute of Astronomy and Astrophysics; [5] CAS -Key Laboratory of FAST, National Astronomical Observatories; [6] National Astronomical Observatories, Chinese Academy of Sciences; [7] Department of Physics, National Tsing Hua University; [8] Institute for Astronomy, National Tsing Hua University; [9] Department of Astronomy, University of Virginia; [10] Center for Astrophysics | Harvard & Smithsonian

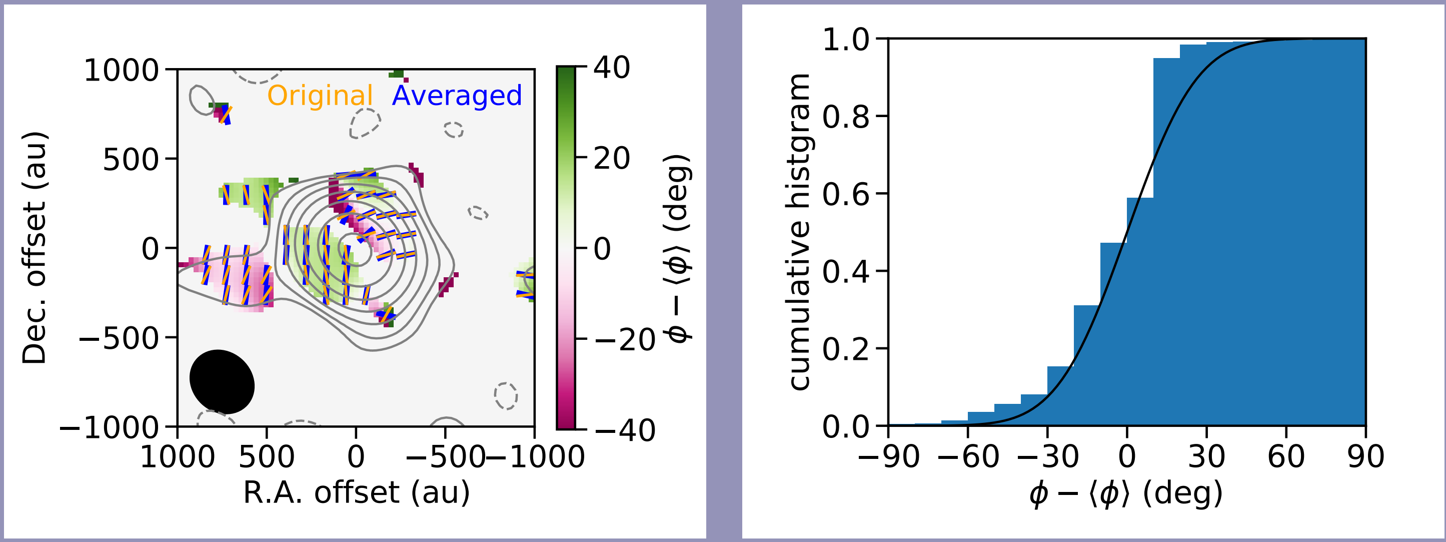

Figure 2: The SMA polarization direction Φ compared with an averaged direction <Φ> smoothed over a Gaussian function with FWHM=6".

studies have constrained kinematics well in this protostar using interferometers: the Keplerian disk (Harsono et al. 2014; Aso et al. 2015), the infalling envelope (Aso et al. 2015), and the molecular outflow (Bjerkeli et al. 2016). In particular, the Keplerian rotation constrains a central stellar mass of 0.5-0.7 $M_{\odot}$ from radial profiles of the rotational velocity derived from the $C^{18}O$ J=2-1 line emission (Harsono et al. 2014; Aso et al 2015). Aso et al. (2015) also estimated a radial infall velocity in the envelope, on the few hundreds au scale, to be ~0.3 times the free fall velocity that was calculated from the central stellar mass, by comparing the $C^{18}O$ emission with a model consisting of a Keplerian disk surrounded by an envelope with the infall velocity uniformly reduced from the free fall velocity. Furthermore, the authors suggested that, if the discrepancy between the estimated infall velocity and the free fall velocity is attributed to a magnetic effect, the infall velocity requires a magnetic-field strength of ~2 mG.

The magnetic effect on the infall velocity in the protostar TMC-1A must be verified by polarization observations that can trace the associated magnetic field. For this purpose, we have observed TMC-1A in the linearly polarized continuum emission at 1.3 mm using the SMA and the Atacama Large Millimeter/submillimeter Array (ALMA). The SMA observations have an angular resolution of ~3" (~400 au at the TMC-1A distance) and a sensitivity of 0.26 mJy/beam for the Stokes Q and U emission , while the ALMA observations have a ~0".3 (~40 au) resolution and a sensitivity of ~0.025 mJy/beam.

Figure 1 shows the polarization fraction and the polarization direction observed in the SMA observations, overlapped with the Stokes I emission. On the few hundreds au scale, the polarization is dominated by the grain alignment along magnetic fields, compared to other polarization mechanisms, such as the self-scattering or the radiative alignment. Hence, the direction of the magnetic field in TMC-1A can be inferred from the polarization direction rotated by 90°, as shown in the right panel of Figure 1. The inferred field direction is not parallel to the major axis of the TMC-1A disk (P.A.=75° or ENE-WSW) or perpendicular. With this direction, the magnetic field can affect gas motion in the envelope near the midplane of this system. In addition, Figure 1 also shows a de-polarized layer from the northeast to the center. This de-polarization can be explained by cancelling out between polarized emission in the orthogonal directions because the field direction is in fact different above and below the de-polarized layer.

The two-dimensional distribution of the magnetic field direction enables us to estimate the field strength on the plane of the sky through the Davis-Chandrasekhar-Fermi (DCF) method (Davis 1951; Chandrasekhar & Fermi 1953). This method requires a mean density, velocity dispersion, and dispersion of the magnetic-field direction, to calculate the field strength. The mean density is estimated to be (0.5-3)×10^{-17} g cm^{-3} from the Stokes I emission observed in our SMA observations. The velocity dispersion is assumed to be, 0.3-1.0 km s^{-1}, between that of $C^{18}O$ emission and the sound speed at a temperature of 28 K (Chandler et al. 1998). The direction dispersion is estimated from our SMA polarization observations. We define an averaged direction by convolving the Stokes Q and U emissions over a Gaussian function with FWHM=4".5-12". Then, the direction dispersion is measured from the averaged direction. Figure 2 shows the difference between the original and averaged directions on the plane of the sky and the cumulative histogram of the direction difference. As a result, the direction dispersion is estimated to be 10°-30°. Finally, the DCF method provides the field strength of 1-5 mG. This is consistent with the value suggested by Aso et al. (2015) in order to explain the infall velocity ~0.3 times the free fall velocity.

The polarized emission observed with the SMA traces a different component from that observed with the ALMA observations at the same wavelength. The ALMA result is interpreted as polarization due to the self-scattering in the central 100 au region and one due to the magnetic alignment along a toroidal field. This difference indicates that our SMA and ALMA observations are complementary to each other.

In conclusion, our SMA observations toward the Class I protostar TMC-1A revealed the magnetic field with a direction between parallel and perpendicular to the disk axis and a strength on the order of mG. These results support the possibility that the magnetic field causes the infall velocity in the associated envelope to be slower than the free fall velocity. The SMA observations trace a different component from our ALMA observations on scales ten times smaller. Further details of this work is published in Aso et al. (2021).

REFERENCES

- Aso, Y., Kwon, W., Hirano, N., et al. 2021, ApJ, 920, 71
- Aso, Y., Ohashi, N., Saigo, K., et al. 2015, ApJ, 812, 27
- Bjerkeli, P., van der Wiel, M. H. D., Harsono, D., et al. 2016, Natur, 540, 406
- Chandler, C. J., Barsony, M., & Moore, T. J. T. 1998, MNRAS, 299, 789
- Chandrasekhar, S., & Fermi, E. 1953, ApJ, 118, 113
- Davis, L. 1951, PhRv, 81, 890
- Galli, P. A. B., Loinard, L., Ortiz-Léon, G. N., et al. 2018, ApJ, 859, 33
- Harsono, D., Jørgensen, J. K., van Dishoeck, E. F., et al. 2014, A&A, 562, A77
- Kristensen, L. E., van Dishoeck, E. F., Bergin, E. A., et al. 2012, A&A, 542, A8
- Maury, A. J., Girart, J. M., Zhang, Q.-Z., et al. 2018, MNRAS, 477, 2760

UTILIZING SWARM TO SHED LIGHT ON THE ORIGIN OF COMPLEX ORGANIC MOLECULES IN STAR-FORMING REGIONS

S.J. van der Walt,[1] L.E. Kristensen,[1] J.K. Jørgensen,[1] H. Calcutt,[2,3] S. Manigand,[1] M. el Akel,[4,1] R.T. Garrod,[5] and K. Qiu[6,7]

INTRODUCTION

Stars form deep inside molecular clouds. These clouds consist primarily of molecular hydrogen, H_2, Helium, and 1% dust by mass. Although the dust clearly does not play a major role in the total mass budget, it is incredibly important when it comes to setting the chemical composition of these clouds: it is on the surfaces of these grains that the bulk of molecules are formed, including H_2. The grain surfaces also play a major role in determining how complex species can form: as molecules such as CO freeze out onto the grains, a chain of reactions is set in motion. First, CO is successively hydrogenated to form the simplest complex organic molecule (a complex organic molecule, COM, is typically defined to have at least 6 atoms, one of which is carbon), methanol (CH_3OH).

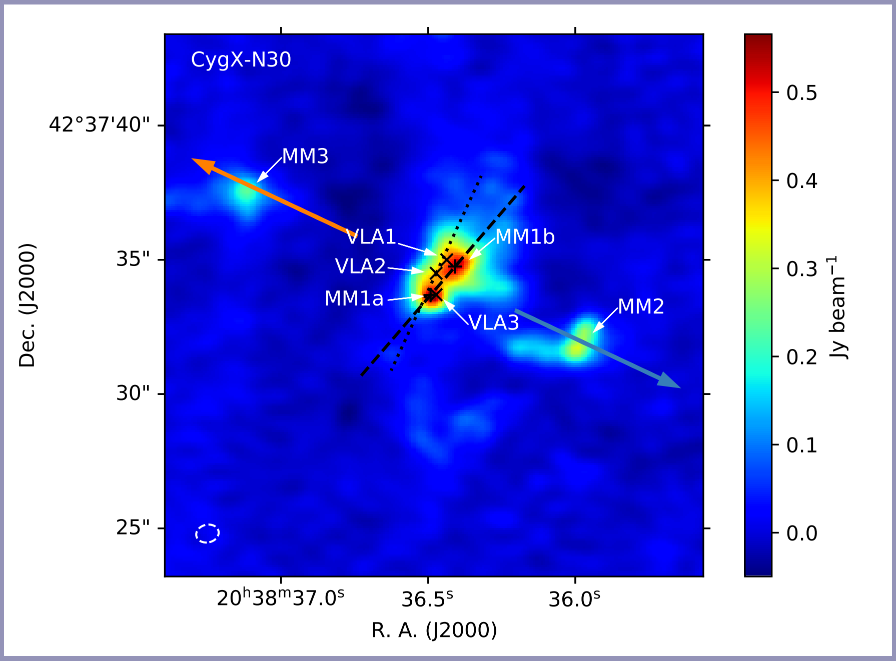

Figure 1: 870 μm continuum image of the N30 region. The positions of three VLA sources are shown (VLA1, 2, and 3; cross symbols) along with the four mm-sources (MM1a and b, MM2, and MM3; plus symbols). The outflow direction is marked with a red and blue arrow. The synthesized beam is shown in the lower left corner with a dashed ellipsoid.

[1]Niels Bohr Institute & Center for Star and Planet Formation, University of Copenhagen; [2]Department of Space, Earth and Environment, Chalmers University of Technology; [3]Institute of Astronomy, Faculty of Physics, Astronomy and Informatics, Nicolaus Copernicus University; [4]CY University, Observatoire de Paris, CNRS, LERMA; [5]Departments of Astronomy and Chemistry, University of Virginia; [6]School of Astronomy and Space Science, Nanjing University; [7]Key Laboratory of Modern Astronomy and Astrophysics (Nanjing University)

Methanol may then react with other molecules on the grains to form ever-more complex species, up to and including simple sugars (Jørgensen et al. 2012) and other potentially pre-biotic molecules. As the grains fall toward the central protostar, they heat up (T $\gtrsim$ 100 K), and the ices sublimate and the molecules are released into the gas phase where they can be observed at (sub)millimeter wavelengths (Herbst & van Dishoeck 2009; Jørgensen et al. 2020) with, e.g., the SMA. Such regions, rich in COM emission, are known as "hot cores". However, this is not the only way in which molecules can enter the gas phase. Alternatives include sputtering of ices in outflows (e.g., Lefloch et al. 2017), shocks as the infalling envelope encounters the protostellar disk (e.g., Artur de la Villarmois et al. 2018), explosive events (e.g., Orozco-Aguilera et al. 2017), or UV photodesorption at the outflow cavity walls (e.g., Drozdovskaya et al. 2015). Which of these processes dominate in releasing the molecules from the ice to the gas phase is in many cases unclear, as is the impact on the observed chemistry.

To understand how molecules are released into the gas phase and any possible impact on the chemistry, the first step is to obtain an inventory of which molecules are present and in what quantity. To do that, rotational transitions of molecules are observed at (sub)millimeter wavelengths, where most of these heavy molecules have transitions and where their line emission is bright. Traditionally, most telescopes covered a limited frequency range, and so a trade-of had to be made: either observe a narrow frequency range and a lot of sources, or a broader frequency range but fewer sources. With the introduction of the new broadband receivers and the SWARM correlator at the SMA, this game was changed: in 2017 it became possible to observe a broad frequency range in one spectral setup, making it observationally inexpensive to obtain these molecular inventories for many sources. Moreover, these can be observed with arcsec resolution, allowing us to pinpoint the spatial origin of emission toward these sources, which is necessary for addressing the physical and chemical origin of the emission.

OBSERVATIONS AND RESULTS

To take advantage of these new capabilities in addressing the origin of gas-phase COMs, we set out to observe 10 intermediate- and high-mass protostars in the nearby (d ~ 1.3 kpc; Rygl et al. 2012) Cygnus-X star-forming region. The frequency range was from 329 – 361 GHz, thus similar to the Protostellar Interferometric Line Survey (PILS, Jørgensen et al. 2016) carried out at ALMA. The sources were observed in a combination of the compact and extended configurations with the SMA, at a resolution of ~ 1". The sources were observed in such a manner that the sensitivity is uniform across the sample. The largest variation in sensitivity is seen across the spectral range of a receiver, and it is 0.2–0.7 Jy

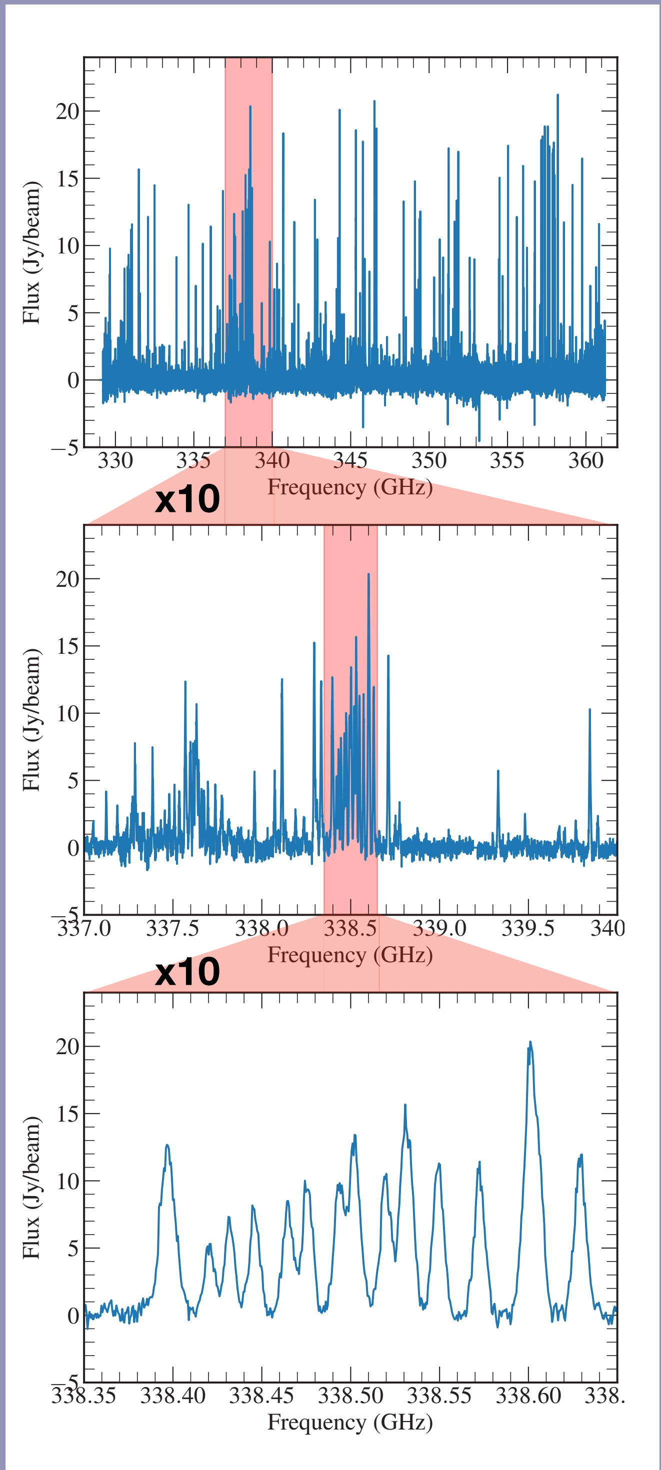

Figure 2: Spectrum obtained toward the N30-MM1a continuum peak. The complete spectrum covers 32 GHz, and each panel provides a zoom-in of a factor of 10 in frequency space. The complete spectrum contains approximately 400 lines from 29 different species. The bottom panel shows bright highly excited CH_3OH emission from the 7k–6k branch.

beam^{-1} in 0.5 km s–1 channels. The first results of this program focused on observations of the bright source W75 N(B), also known as CygX-N30 (Motte et al. 2007; Minh et al. 2010), were recently published in van der Walt et al. (2021, A&A, in press) and are reported here. We also refer the reader to this paper for the full details on the observing strategy and observing details.

The dust continuum is shown in Fig. 1. The previously identified continuum sources are marked, as are the VLA sources. The gas + dust mass of the bright MM1a and b sources is ~3 $M_\odot$ for each source.

The full spectrum obtained toward the MM1a source is shown in Fig. 2. Each panel of the figure provides a magnification of a factor of 10, thereby illustrating the spectral coverage. Approximately 400 lines were detected originating in 29 different species and their isotopologues. They range from simple molecules such as CO to complex organic molecules (CH_3OH, C_2H_5OH, CH_3OCH_3, CH_3OCHO, and CH_3CN). The molecular emission can be put in two categories: either the emission is extended along a north-south gradient, where an analysis of position-velocity diagrams suggest that the origin is in an infalling-rotating structure (Zhu et al. 2011). This type of behavior is typically traced by emission from simpler mol-

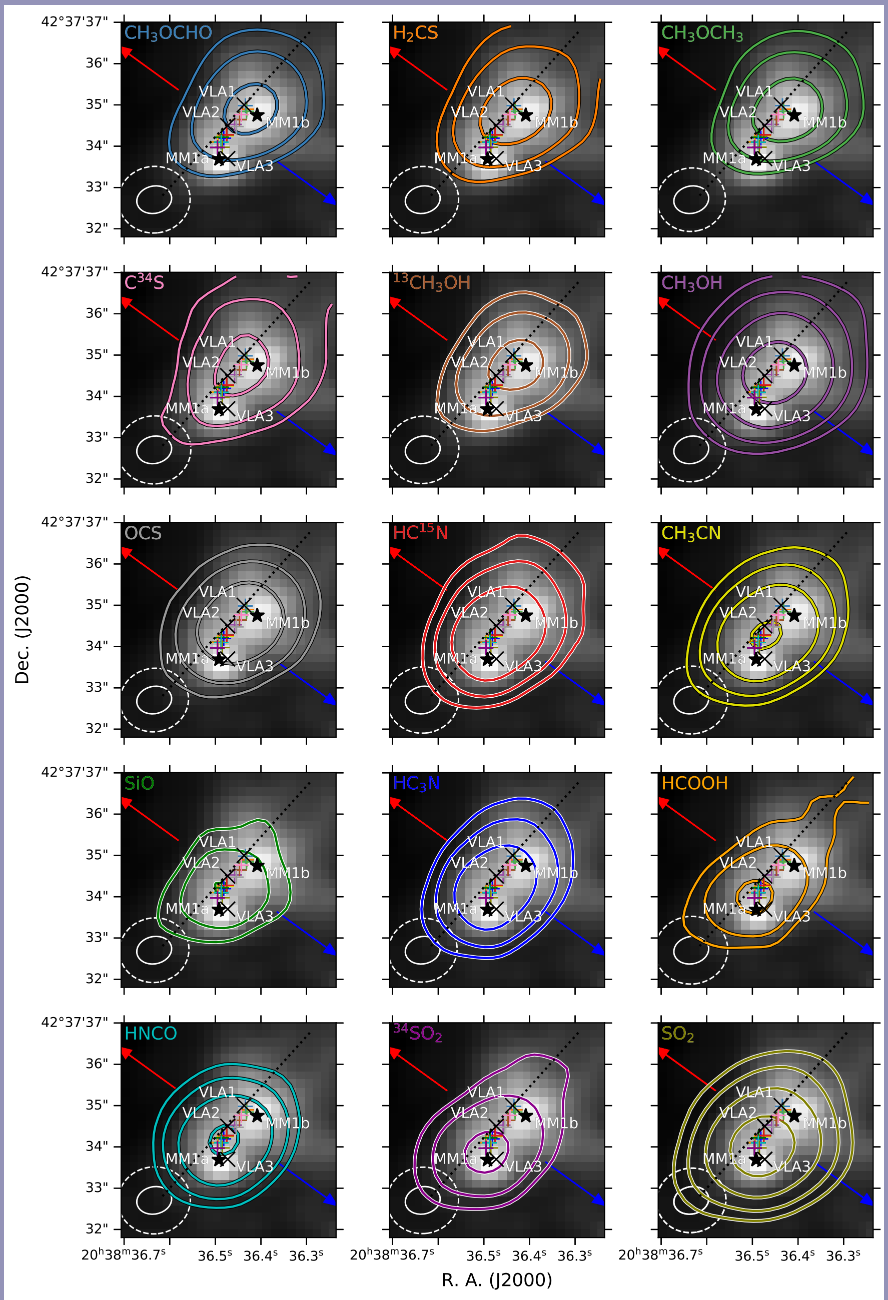

Figure 3: Emission of selected species (contours) overlaid on the continuum (greyscale). The molecular peak positions are marked with colored plus symbols of the same color as the respective molecule contour plot. The positions of MM1a and b are marked with stars, and the outflow direction is marked with a red and blue arrow. The contours are in steps of 3, 6, 12, 24σ. The beam for line emission is shown in a dashed ellipsoid while the continuum is shown in full.

ecules, e.g., CS and H_2CO. Emission from the more complex species is typically unresolved at the resolution of 1".

The emission peaks of the unresolved emission do not originate from the same position. Instead there is a gradient, where the emission from CH_3OCH_3, CH_3OCHO, H_2CS, and C_2H_5OH peaks north of MM1b. CH_3OH, OCS, and CS peak between the two continuum sources. Finally, the emission from CH_3CN, $H_{13}CN$, HC_3N, HNCO, HCOOH, SiO, and SO_2 peaks south of MM1a. This is illustrated in Fig. 3, where the gradient is seen to extend over more than $\gtrsim$ 1", or ~ 1300 AU at the distance of this source. These different peaks do not overlap directly with the continuum sources, but appear to offset from them. These differences in emission cannot be attributed to excitation effects, nor to dust opacity effects.

ORIGIN OF EMISSION?

Emission from COMs is most often interpreted as coming from a hot core. In this scenario the grains fall toward the protostar, are heated, and all ices sublimate into the gas phase where we observe them. Thus, we would expect to see the emission peaking in the same place and near the protostar. This scenario can, however, clearly be ruled out: the different species do not peak in the same location, nor is emission directly associated with the protostars. Furthermore, the gradient is observed to be perpendicular to the outflow, which suggests that this is not the source of the emission. Similarly, it is unlikely that the emission originates from UV photodesorption along the outflow cavity walls for the same reasons.

Instead, it appears that the origin of emission is linked to the infalling rotating structure ("disk") traced by, e.g., H_2CO and CS. In this scenario, the O-bearing COM emission is likely caused by a combination of processes, including accretion of infalling material onto the disk surface, while the N- and S-bearing species towards VLA3/MM1a might be a slightly more evolved source where the gas-phase chemistry had more time to evolve. This type of differentiation is beginning to be observed toward more and more sources (e.g., Allen et al. 2017; Csengeri et al. 2018), illustrating that hot cores are not just hot cores.

These observations demonstrate the need of observing large frequency ranges at high angular resolution in one go in order to shed light on the physical and chemical origin of COMs. The broad frequency range is needed to cover a large number of transitions, so that the excitation conditions can be inferred. The high spatial resolution ensures that spatial correlation (or not) can be examined in detail. This is particularly important for intermediate- and high-mass protostellar sources, where the physical structure is complex. Therefore, it complicates our understanding of the origin of the emission. Further analysis of the remaining nine sources in the sample will certainly continue to inform us of the origin of COM emission

REFERENCES

- Allen, V., van der Tak, F. F. S., Sa´nchez-Monge, A.,´ Cesaroni, R., & Beltra´n, M. T. 2017, A&A, 603, A133, doi: 10.1051/0004-6361/201629118
- Artur de la Villarmois, E., Kristensen, L. E., Jørgensen, J. K., et al. 2018, A&A, 614, A26, doi: 10.1051/0004-6361/201731603
- Csengeri, T., Bontemps, S., Wyrowski, F., et al. 2018, A&A, 617, A89, doi: 10.1051/0004-6361/201832753
- Drozdovskaya, M. N., Walsh, C., Visser, R., Harsono, D., & van Dishoeck, E. F. 2015, MNRAS, 451, 3836, doi: 10.1093/mnras/stv1177
- Herbst, E., & van Dishoeck, E. F. 2009, ARA&A, 47, 427, doi: 10.1146/annurev-astro-082708-101654
- Jørgensen, J. K., Belloche, A., & Garrod, R. T. 2020, ARA&A, 58, 727, doi: 10.1146/annurev-astro-032620-021927
- Jørgensen, J. K., Favre, C., Bisschop, S. E., et al. 2012, ApJL, 757, L4, doi: 10.1088/2041-8205/757/1/L4 Jørgensen, J. K., van der Wiel, M. H. D., Coutens, A., et al. 2016, A&A, 595, A117, doi: 10.1051/0004-6361/201628648
- Lefloch, B., Ceccarelli, C., Codella, C., et al. 2017, MNRAS, 469, L73, doi: 10.1093/mnrasl/slx050
- Minh, Y. C., Su, Y. N., Chen, H. R., et al. 2010, ApJ, 723, 1231, doi: 10.1088/0004-637X/723/2/1231
- Motte, F., Bontemps, S., Schilke, P., et al. 2007, A&A, 476, 1243, doi: 10.1051/0004-6361:20077843
- Orozco-Aguilera, M. T., Zapata, L. A., Hirota, T., Qin, S.-L., & Masqu´e, J. M. 2017, ApJ, 847, 66, doi: 10.3847/1538-4357/aa88cd
- Rygl, K. L. J., Brunthaler, A., Sanna, A., et al. 2012, A&A, 539, A79, doi: 10.1051/0004-6361/201118211
- van der Walt, S. J., Kristensen, L. E., Jørgensen, J. K., et al. 2021, A&A, 665, 86, doi: 10.1051/0004-6361/202039950
- Zhu, L., Zhao, J.-H., & Wright, M. C. H. 2011, ApJ, 740, 114, doi: 10.1088/0004-637X/740/2/114

STATUS OF NEW CRYOSTAT FOR wSMA

Edward Tong, Paul Grimes and Lingzhen Zeng

SMA staff have been working with High Precision Devices (acquired by Form Factor in 2020) to develop a prototype cryostat for the wSMA upgrade, which we have described in a previous article[1]. Two such cryostats have been delivered, the second of which now meets all of the SMA cryogenic requirements.

We have performed extensive testing of both prototypes, not only in terms of cooling capacity and cooldown times, but also of the optical alignment of critical elements within the cryostat. At the right are two photographs of the second prototype, which delivers a base temperature of 4.0 K, and fully meets our target alignment specifications.

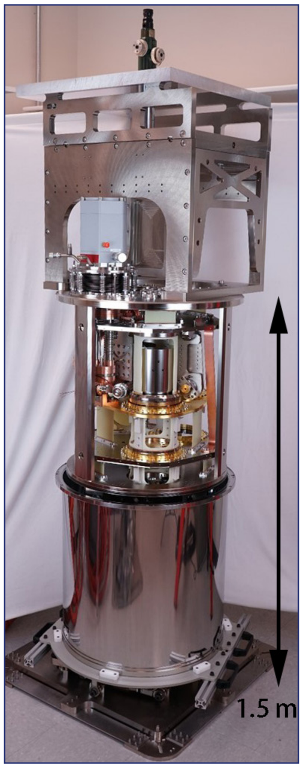

Each of the prototypes houses two receiver cartridges, one for the Low Band (LO coverage 210-270 GHz) and one for the High Band (LO coverage 280-360 GHz). An initial Low Band receiver cartridge has been assembled, carrying the dual polarization front-end assembly and a pair of mixer blocks, one for each polarization, and laboratory testing of this cartridge has begun. Work on assembling the first of the High Band receiver cartridges has begun and we expect to make cryogenic measurements of this alongside the Low Band cartridge in the coming months.

Having procured two prototype cryostats, we are developing plans to ship one to the SMA site on Maunakea to check mechanical interfaces, to verify optical alignment, and to evaluate the performance of first of the Low Band receivers.

[1] Paul Grimes et al, "Introducing the wSMA – a major upgrade to the SMA receiver systems," SMA Newsletter, p 17-19, Jan. 2017. https://lweb.cfa.harvard.edu/sma/Newsletters/pdfFiles/SMA_NewsJan2017.pdf

2022 SUBMILLIMETER ARRAY INTERFEROMETRY SCHOOL

The Center for Astrophysics, in conjunction with the Academia Sinica Institute of Astronomy and Astrophysics and the University of Hawaii, is organizing the 3rd annual Submillimeter Array Interferometry School, to be held virtually online from 18-22 January 2022. The main goals of the school are to provide graduate students, post-docs and scientists outside the field with a broad knowledge of interferometry and data reduction techniques at (sub)millimeter wavelengths.

The workshop will provide a series of lectures focusing on fundamentals of radio interferometry, with a special emphasis on the Submillimeter Array (SMA) interferometer and its new capabilities. The school will also extensively utilize the SMA, located on Maunakea, providing hands-on experience of actively performing observations and data reduction for projects proposed by school participants. Lecture material from the school will be made available through the SMA School website, following the conclusion of the school.

Website: www.cfa.harvard.edu/sma-school

Contact: sma-school@cfa.harvard.edu

CALL FOR STANDARD OBSERVING PROPOSALS - 2022A SEMESTER

We wish to draw your attention to the next Call for Standard Observing Proposals for observations with the Submillimeter Array (SMA). This call is for the 2022A semester with observing period **16 May 2022 - 15 Nov 2022.**

Standard Observing Proposals Submission deadline: **Thursday, 3 March 2022 21:00 UTC**

The full Call for Proposals, with details on time available and the proposal process, will be available by January 29 at the SMA Observer Center (SMAOC) at **http://sma1.sma.hawaii.edu/call.html.**

Details on the SMA capabilities and status can be found at **http://sma1.sma.hawaii.edu/status.html;** proposal creation and submission is also done through the SMAOC at **http://sma1.sma.hawaii.edu/proposing.html.** We are happy to answer and questions and provide assistance in proposal submission, simply email sma-propose@cfa.harvard.edu with any inquiries.

Sincerely,

Mark Gurwell
SAO Chair, SMA TAC

Hau-Yu (Baobab) Liu
ASIAA Chair, SMA TAC

STAFF CHANGES

Andrea Waiters, Astrophysicist (Telescope Operator), joined SAO in August, reporting to Ram Rao. She recently earned her bachelor's degrees in astronomy and in physics at the University of Hawai'i at Hilo.

John Lopez, Astrophysicist (Telescope Operator), joined SAO in November, reporting to Ram Rao. He recently earned his bachelor's degree in astrophysics at the University of California at Santa Cruz.

Austin Jennings, Astrophysicist (Telescope Operator), left the SMA at the end of August to pursue other opportunities. We thank Austin for his efforts and wish him success in the future.

Christopher Moriarty, computer engineer, moved to a new CfA software engineering leadership position with SAO Central Engineering on November 1. Since his move from STSci to the CfA three years ago, Chris has made countless contributions towards improving SMA systems and operations. We are very grateful that he will be continuing on as our CfA colleague.

PROPOSAL STATISTICS 2021B (2021 NOV 16 - 2022 MAY 15)

The three SMA partner institutions received a total of 71 proposals (SAO 55, ASIAA 13, UHawaii 3) requesting observing time in the 2021B semester. The 71 proposals were divided among science categories as follows:

CATEGORY	PROPOSALS
local galaxies, starbursts, AGN	13
protoplanetary, transition, debris disks	12
submm/hi-z galaxies	12
low/intermediate mass star formation, cores	11
high mass (OB) star formation, cores	10
GRB, SN, high energy	5
evolved stars, AGB, PPN	3
Galactic Center	3
other	1

TRACK ALLOCATIONS BY WEATHER REQUIREMENT AND CONFIGURATION (ALL PARTNERS):

Note that after the 2021B proposal deadline, it was concluded by the technical and management teams that a multiweek pause of science operations was needed in 2021B to address several long term maintenance and system upgrade projects. This pause is scheduled for the period 31 January - 25 February 2022 (with a contingency extendable to 5 March). It was furthermore decided to limit the number of configurations for the semester to two, one prior to the pause, and one after. To best accomodate the highest ranked programs from each of the partners, it was determined that the configurations would be compact (16 Nov 2021 - 30 Jan 2022) and extended (26 Feb 2022 - 15 May 2022), reconfiguration occurring during the science pause.

PWV[1]	SAO	ASIAA	UH[2]
< 4.0mm	40A + 25B	3A + 13B	0
< 2.5mm	10A + 22B	9A + 5B	18
< 1.0mm	0A + 1B	1A + 0B	0
Total	**50A + 48B**	**13A + 18B**	**18**

Configuration	SAO	ASIAA	UH[2]
Compact	11A + 20B	5A + 7B	16
Extended	30A + 19B	1A + 0B	2
Either	9A + 9B	7A + 11B	0
Total	**50A + 48B**	**13A + 18B**	**18**

(1) Precipitable water vapor required for the observations.
(2) UH does not list As and Bs.

TOP-RANKED 2021B SEMESTER PROPOSALS

The following is the listing of all SAO, ASIAA, and UH proposals with at least a partial A ranking with the names and affiliations of the principal investigators.

GALACTIC CENTER

Sara Issaoun, CfA
Probing Black Hole Accretion Flows with Faraday Rotation

Garrett "Karto" Keating, CfA
Polarimetric VLBI for the 2022 Event Horizon Telescope Campaign

GRB, SN, HIGH ENERGY

Joe Bright, UC Berkeley
Constraining the Nature and Progenitors of the Fast Blue Optical Transients

Anna Ho, UC Berkeley
The Landscape of Relativistic Stellar Explosions

Yuji Urata, NCU
Electro-magnetic wave candidate of IceCube Neutrino event

HIGH MASS (OB) STAR FORMATION, CORES

Qizhou Zhang, CfA
Magnetic Fields and protocluster formation

LOCAL GALAXIES, STARBURSTS, AGN

Venkatessh Ramakrishnan, University of Concepcion, CL
Polarimetric monitoring of the flaring blazar 1156+295

Gerrit Schellenberger, CfA
Understanding the Time Variability of the AGN in NGC 5044

Steven Willner, CfA
Disentangling radiating particle properties and jet physics from M87 multi-wavelength variability (copied from 2021A-S047)

LOW/INTERMEDIATE MASS STAR FORMATION, CORES

Jennifer Bergner, University of Chicago
Molecular mapping of the chemically rich outflow B1-a

Andrew Burkhardt, Wellesley College
Resolving the Redshifted Outflow in the New Chemically-Active Outflow HH114: Is There a Precessing Jet, Episodic Ejection(s), or Both?

Naomi Hirano, ASIAA
Magnetic fields in the central regions of prestellar cores

Dipen Sahu, ASIAA
Stability of centrally dense prestellar cores at a scale of 2000 AU

PROTOPLANETARY, TRANSITION, DEBRIS DISKS

Sean Andrews, CfA
Disk Evolution using the "Distributed" Taurus Population

Chia-Ying Chung, ASIAA
A statistical study to constrain grain growth efficiency in protoplanetary disks

Feng Long, CfA
Mapping the Gas Environment of Heavily Veiled Young Stars

Suchitra Narayanan, IAA/UH
Search for sulfur organics in embedded disks in the Taurus molecular region

Richard Teague, CfA
Is the Magneto-Rotational Instability Driving Protoplanetary Disk Evolution?

Jonathan Williams, IAA/UH
Do disks clear out gradually or suddenly?

SUBMM/HI-Z GALAXIES

Lennox Cowie, IAA/UH
A uniquely massively star-forming protocluster at z=3.15 in the GOODS-N

Zhen-Kai Gao, ASIAA
SMA STUDIES IV: SCUBA-2 450μm Close Pairs

SOLAR SYSTEM

Nathan Roth, NASA GSFC
A Search for Distributed Sources at Small Heliocentric Distance in Comets C/2021 A1 (Leonard) and C/2021 O3 (PanSTARRS)

STANDARD AND LARGE SCALE PROJECTS OBSERVED DURING 2021A

SMA Semester 2021A encompassed the period Jun 1 – 11 Nov 2021. The start of the semester was delayed by two weeks due to hardware failures for two antennas and the transporter during March. These problems persisted into 2021A, leading to only six antennas being available until late August, and cancelation of the first EXT configuration. The small number of antennas for COM was ameliorated by observing selected COM projects in each of two hybrid 6-antenna configurations; when combined the two provided effectively the same sensitivity and UV coverage as a single observation with an 8-antenna COM array. Unavoidably, this caused significant operational inefficiency, since each project required twice the number of observations. Further, new transporter faults occurred in early October, causing cancelation of the second EXT configuration as well as VEX. Nonetheless, it was a successful semester with many completed projects. In addition, one SAO large scale program was allocated significant time in September/early October.

Listed below are all SMA standard, DDT and large scale projects that were at least partially completed during the SMA Semester 2021A.

EVOLVED STARS, AGB, PPN

Cristobal Bordiu, Istituto Nazionale di Astrofisica (INAF)
Peering into the heart of the luminous blue variable MWC 930

Nimesh Patel, CfA
Chemical Evolution from AGB to PN: A Spectral-line Survey of the Egg Nebula

GRB, SN, HIGH ENERGY

Deanne Coppejans, Northwestern University
Constraining the Nature and Progenitors of the Fast Blue Optical Transients

Yuji Urata, NCU
Electro-magnetic wave candidate of IceCube Neutrino event

HIGH MASS (OB) STAR FORMATION, CORES

Henrik Beuther, MPIA
The importance of magnetic fields for the fragmentation of high-mass star-forming regions (the remaining targets)

Yue Cao, CfA
70-um-dark cores: a new window to the initial condition of massive star formation

Ivalu Barlach Christensen, MPIfR
The Excitation of Deuterated Dense Cores in the Spine of the Swan, DR21

Hao-Yuan Duan, National Tsing Hua University
Magnetic fields associated with a network of filaments in massive star-forming region Onsala 2

Pamela Freeman, University of Calgary
Where are the Carbon Chain Molecules in DR21(OH)?

Han-Tsung Lee, ASIAA/NCU
Magnetic field in fragmented cores

Junhao Liu, EAO
A pilot dust polarization survey of massive dense cores in Cygnus-X

Tatiana Rodriguez, New Mexico Institute of Mining and Technology
The Jet-Flow Relation in the High-Mass Star-Forming Region IRAS 19411+2306

Qizhou Zhang, CfA
Magnetic Fields and protocluster formation

LOCAL GALAXIES, STARBURSTS, AGN

Mathew Ashby, CfA
Measuring H2 Conversion Factors and Physical Conditions in GMCs

Mojegan Azadi, CfA
The Emission Mechanisms in Radio Galaxies at the Peak of Star Formation Activity of the Universe

Tirna Deb, Kapteyn Astronomical Institute, University of Groningen, NL
SYMPHANY: SYnergy of Molecular PHase And Neutral hYdrogen in galaxies in Abell 2626

Deanne Fisher, Swinburne University
Testing Feedback Theory in Starbursting Disk Galaxies

Jan Forbrich, U Hertfordshire
SMA Survey of Resolved Dust and Simultaneous CO Observations of GMCs in M31 [Large Scale Program]

Eric Koch, CfA
A resolved molecular gas survey of the edge-on galaxy NGC 891

Glen Petitpas, CfA
The Beautiful and Enigmatic Spiral Galaxy NGC 7331

Venkatessh Ramakrishnan, University of Concepcion, CL
Polarimetric monitoring of the flaring blazar 1156+295

Gerrit Schellenberger, CfA
Understanding the Time Variability of the AGN in NGC 5044

Steven Willner, CfA
Disentangling radiating particle properties and jet physics from M87 multi-wavelength variability

LOW/INTERMEDIATE MASS STAR FORMATION, CORES

Nacho Anez, Institut de Ciències de l'Espai (ICE, IEEC-CSIC)
Linking fragmentation with the evolutionary stage in twin hubs in the IRDC G14.225-0.506

Andrew Burkhardt, Wellesly College
Resolving the Redshifted Outflow in the New Chemically-Active Outflow HH114: Is There a Precessing Jet, Episodic Ejection(s), or Both?

Logan Francis, University of Victoria
Completing SMA Monitoring of the periodic outbursting protostar EC53

Chat Hull, NAOJ
Cepheus Polarization Pilot Survey

Natsuko Izumi, ASIAA
Filament structure in low-metallicity environment

Chin-Fei Lee, ASIAA
Searching for outflows in a very short time-scale sporadic-accretion brown dwarf

Maria Maureira, MPE
Uncovering the true nature of a highly evolved cold core in the Aquila rift

Carlos Eduardo Munoz-Romero, Harvard University/CfA
Resolving the Chemical Evolution of Class 0/I Protostars in Perseus

Goran Sandell, IAA/UH
Young outflows and outflow sources south of DR21

Maria Teresa Valdivia Mena, MPE
Measuring the full length of the streamer feeding a Class I protostar in NGC 1333

PROTOPLANETARY, TRANSITION, DEBRIS DISKS

Chian-Chou Chen, ASIAA
A statistical study to constrain grain growth efficiency in protoplanetary disks

Chia-Ying Chung, ASIAA
A statistical study to constrain grain growth efficiency in protoplanetary disks

Charles Law, Harvard University/CfA
Connecting scaling laws between exoplanets and young disks

Feng Long, CfA
Mapping the Gas Environment of Heavily Veiled Young Stars

Charlie Qi, CfA
Resolving the gas vertical structure of edge-on protoplanetary disks

Abygail Waggoner, University of Virginia
Was Variable Ion Chemistry in the Im Lup Planet-Forming Disk Caused by Stellar X-Ray Flares?

SUBMM/HI-Z GALAXIES

Jaclyn Champagne, University of Texas at Austin
Searching for the Cores of the Most Massive Galaxy Protoclusters at $2<z<3$

David Clements, Imperial College London
The Nature of SPIRE dropouts - ultrahigh redshift, cold dust or what?

Giovanni Fazio, CfA
Understanding the Evolution of Obscured Activity Over Cosmic Time: A Pilot Survey in the JWST Time Domain Field

Kevin Harrington, ESO/Chile
Rest-frame 775 - 1730 GHz ISM Diagnostics of the Most IR Luminous, Lensed Planck Starburst at $z = 3$

William Schap, University of Florida
Characterizing the disk fraction of M dwarfs

Antony Stark, CfA
First Radio Observations of the Brightest Known Object at $z > 5$

Richard Teague, CfA
A 3D Exploration of an Edge-On Self-Gravitating Disk

Qizhou Zhang, CfA
Magnetic Fields and protocluster formation

RECENT PUBLICATIONS

TITLE: Magnetic field strengths of the synchrotron self-absorption region in the jet of CTA 102 during radio flares
AUTHOR: Kim, S.-H., Lee, S.-S., Lee, J. W., Hodgson, J. A., Kang, S., Algaba, J.-C., Kim, J.-Y., Hodges, M., Agudo, I., Fuentes, A., Escudero, J., Myserlis, I., Traianou, E., Lähteenmäki, A., Tornikoski, M., Tammi, J., Ramakrishnan, V., Järvelä, E.
PUBLICATION: *Monthly Notices of the Royal Astronomical Society, 510, 815-833*
PUBLICATION DATE: 02/2022
ABSTRACT: https://ui.adsabs.harvard.edu/abs/2022MNRAS.510..815K
DOI: 10.1093/mnras/stab3473

TITLE: A double-period oscillation signal in millimeter emission of the radio galaxy NGC 1275
AUTHOR: Zhang, P., Wang, Z., Gurwell, M., Wiita, P. J.
PUBLICATION: *arXiv e-prints, arXiv:2112.03544*
PUBLICATION DATE: 12/2021
ABSTRACT: https://ui.adsabs.harvard.edu/abs/2021arXiv211203544Z

TITLE: On the Origin of Gamma-Ray Flares from Bright Fermi Blazars
AUTHOR: Paliya, V. S., Böttcher, M., Gurwell, M., Stalin, C. S.
PUBLICATION: *The Astrophysical Journal Supplement Series, 257, 37*
PUBLICATION DATE: 12/2021
ABSTRACT: https://ui.adsabs.harvard.edu/abs/2021ApJS..257...37P
DOI: 10.3847/1538-4365/ac365d

TITLE: Evolution and Kinematics of Protostellar Envelopes in the Perseus Molecular Cloud
AUTHOR: Heimsoth, D. J., Stephens, I. W., Arce, H. G., Bourke, T. L., Myers, P. C., Dunham, M. M.
PUBLICATION: *arXiv e-prints, arXiv:2112.09848*
PUBLICATION DATE: 12/2021
ABSTRACT: https://ui.adsabs.harvard.edu/abs/2021arXiv211209848H

TITLE: The evolution of temperature and density structures of OB cluster-forming molecular clumps
AUTHOR: Lin, Y., Wyrowski, F., Liu, H. B., Izquierdo, A., Csengeri, T., Leurini, S., Menten, K. M.
PUBLICATION: *arXiv e-prints, arXiv:2112.01115*
PUBLICATION DATE: 12/2021
ABSTRACT: https://ui.adsabs.harvard.edu/abs/2021arXiv211201115L

TITLE: Protostellar Interferometric Line Survey of the Cygnus X region (PILS-Cygnus). First results: Observations of CygX-N30
AUTHOR: van der Walt, S. J., Kristensen, L. E., Jørgensen, J. K., Calcutt, H., Manigand, S., el Akel, M., Garrod, R. T., Qiu, K.
PUBLICATION: *Astronomy and Astrophysics, 655, A86*
PUBLICATION DATE: 11/2021
ABSTRACT: https://ui.adsabs.harvard.edu/abs/2021A&A...655A..86V
DOI: 10.1051/0004-6361/202039950

TITLE: The disk-outflow system around the rare young O-type protostar W42-MME
AUTHOR: Dewangan, L. K., Zinchenko, I. I., Zemlyanukha, P. M., Liu, S.-Y., Su, Y.-N., Kurtz, S. E., Ojha, D. K., Pazukhin, A. G., Mayya, Y. D.
PUBLICATION: *arXiv e-prints, arXiv:2111.01373*
PUBLICATION DATE: 11/2021
ABSTRACT: https://ui.adsabs.harvard.edu/abs/2021arXiv211101373D

TITLE: The Variability of the Black-Hole Image in M87 at the Dynamical Time Scale
AUTHOR: Satapathy, K., Psaltis, D., Ozel, F., Medeiros, L., Dougall, S. T., Chan, C.-. kwan ., Wielgus, M., Prather, B. S., Wong, G. N., Gammie, C. F., Akiyama, K., Alberdi, A., Alef, W., Algaba, J. C., Anantua, R., Asada, K., Azulay, R., Baczko, A.-K., Ball, D. R., Baloković, M., Barrett, J., Benson, B. A., Bintley, D., Blackburn, L., Blundell, R., Boland, W., Bouman, K. L., Bower, G. C., Boyce, H. A., Bremer, M., Brinkerink, C. D., Brissenden, R., Britzen, S., Broderick, A. E., Broguiere, D., Bronzwaer, T., Bustamente, S., Byun, D.-Y., Carlstrom, J. E., Chael, A., Chatterjee, K., Chatterjee, S., Chen, M.-T., Chen, Y., Cho, I., Christian, P., Conway, J. E., Cordes, J. M., Crawford, T., Crew, G. B., Cruz Osorio, A., Cui, Y., Davelaar, J., De Laurentis, M., Deane, R., Dempsey, J. T., Desvignes, G., Dexter, J., Doeleman, S. S., Eatough, R., Falcke, H., Farah, J. R., Fish, V., Fomalont, E. B., Ford, H. A., Fraga-Encinas, R., Friberg, P., Fromm, C. M., Fuentes, A., Galison, P., García, R., Gentaz, O., Georgiev, B., Goddi, C., Gold, R., Gomez-Ruiz, A. I., Gómez, J. L., Gu, M., Gurwell, M. A., Hada, K., Haggard, D., Hecht, M., Hesper, R., Ho, L. C., Ho, P. T., Honma, M., Huang, C.-W. L., Huang, L., Hughes, D. H., Ikeda, S., Inoue, M., Issaoun, S., James, D. J., Jannuzi, B. T., Janssen, M., Jeter, B., Jiang, W., Jimenez Rosales, A., Johnson, M. D., Jorstad, S. G., Jung, T., Mansour Karami, M., Karuppusamy, R., Kawashima, T., Keating, G. K., Kettenis, M., Kim, D.-J., Kim, J.-Y., Kim, J., Kim, J., Kino, M., Koay, J. Y., Kofuji, Y., Koch, P. M., Koyama, S., Kramer, C., Kramer, M., Krichbaum, T. P., Kuo, C.-Y., Lauer, T. R., Lee, S.-S., Levis, A., Li, Y.-R., Li, Z., Lindqvist, M., Lico, R., Lindahl, G., Liu, J., Liu, K., Liuzzo, M. E., Lo, W.-P., Lobanov, A., Loinard, L., Lonsdale, C. J., Lu, R., MacDonald, N. R., Mao, J., Marchili, N., Markoff, S., Marrone, D., Marscher, A. P., Marti-Vidal, I., Matsushita, S., Matthews, L., Menten, K. M., Mizuno, I., Mizuno, Y., Moran, J., Moriyama, K., Moscibrodzka, M., Muller, C., Mejias, A. M., Musoke, G., Nagai, H., Nagar, N. M., Nakamura, M., Narayan, R., Narayanan, G., Natarajan, I., Nathanail, A., Neilsen, J., Neri, R., Ni, C., Noutsos, A., Nowak, M. A., Okino, H., Olivares, H., Ortiz-Leon, G. N., Oyama, T., Palumbo, D. C., Park, J., Patel, N. A., Pen, U.-L., Pesce, D. W., Pietu, V., Plambeck, R. L., PopStefanija, A., Porth, O., Potzl, F., Preciado-López, J. A., Pu, H.-Y., Ramakrishnan, V., Rao, R., Rawlings, M., Raymond, A. W., Rezzolla, L., Ripperda, B., Roelofs, F., Rogers, A. E. E., Ros, E., Rose, M., Roshanineshat, A., Rottmann, H., Roy, A. L., Ruszczyk, C., Rygl, K., Sanchez, S., Sanchez-Arguelles, D., Sasada, M., Savolainen, T., Schloerb, F. P., Schuster, K.-F., Shao, L., Shen, Z.-Q., Small, D., Sohn, B. W., SooHoo, J., Sun, H., Tazaki, F., Tetarenko, A. J., Tiede, P., Tilanus, R., Titus, M., Toma, K., Torne, P., Traianou, E., Trent, T., Trippe, S., van Bemmel, I., van Langevelde, H. J., van Rossum, D. R., Wagner, J., Ward-Thompson, D., Wardle, J. F., Weintroub, J., Wex, N., Wharton, R., Wiik, K., Wu, Q., Yoon, D., Young, A., Young, K. H., Younsi, Z., Yuan, F., Yuan, Y.-F., Zensus, J. A., Zhao, G.-Y., Zhao, S.-S.
PUBLICATION: *arXiv e-prints, arXiv:2111.01317*
PUBLICATION DATE: 11/2021
ABSTRACT: https://ui.adsabs.harvard.edu/abs/2021arXiv211101317S

TITLE: A Multiwavelength Study of ELAN Environments (AMUSE^2). Mass budget, satellites spin alignment and gas infall in a massive z ~ 3 quasar host halo
AUTHOR: Arrigoni Battaia, F., Chen, C.-C., Liu, H.-Y. B., De Breuck, C., Galametz, M., Fumagalli, M., Yang, Y., Zanella, A., Man, A., Obreja, A., Prochaska, J. X., Bañados, E., Hennawi, J. F., Farina, E. P., Zwaan, M. A., Decarli, R., Lusso, E.
PUBLICATION: *arXiv e-prints, arXiv:2111.15392*
PUBLICATION DATE: 11/2021
ABSTRACT: https://ui.adsabs.harvard.edu/abs/2021arXiv211115392A

TITLE: Radio and gamma-ray activity in the jet of the blazar S5 0716+714
AUTHOR: Kim, D.-W., Kravchenko, E. V., Kutkin, A. M., Böttcher, M., Gómez, J. L., Gurwell, M., Jorstad, S. G., Lähteenmäki, A., Marscher, A. P., Ramakrishnan, V., Tornikoski, M., Trippe, S., Weaver, Z., Williamson, K. E.
PUBLICATION: *arXiv e-prints, arXiv:2111.03006*
PUBLICATION DATE: 11/2021
ABSTRACT: https://ui.adsabs.harvard.edu/abs/2021arXiv211103006K

TITLE: Multi-scale Dust Polarization and Spiral-like Stokes-I Residual in the Class I Protostellar System TMC-1A
AUTHOR: Aso, Y., Kwon, W., Hirano, N., Ching, T.-C., Lai, S.-P., Li, Z.-Y., Rao, R.
PUBLICATION: *The Astrophysical Journal, 920, 71*
PUBLICATION DATE: 10/2021
ABSTRACT: https://ui.adsabs.harvard.edu/abs/2021ApJ...920...71A
DOI: 10.3847/1538-4357/ac15f3

TITLE: Morphological Transition of the Compact Radio Lobe in 3C 84 via the Strong Jet-Cloud Collision
AUTHOR: Kino, M., Niinuma, K., Kawakatu, N., Nagai, H., Giovannini, G., Orienti, M., Wajima, K., DAmmando, F., Hada, K., Giroletti, M., Gurwell, M.
PUBLICATION: *The Astrophysical Journal, 920, L24*
PUBLICATION DATE: 10/2021
ABSTRACT: https://ui.adsabs.harvard.edu/abs/2021ApJ...920L..24K
DOI: 10.3847/2041-8213/ac24fa

TITLE: Multi-Wavelength Study of 4C+28.07
AUTHOR: Das, A. K., Prince, R., Gupta, N.
PUBLICATION: *The Astrophysical Journal, 920, 117*
PUBLICATION DATE: 10/2021
ABSTRACT: https://ui.adsabs.harvard.edu/abs/2021ApJ...920..117D
DOI: 10.3847/1538-4357/ac178c

TITLE: Identifying changing jets through their radio variability
AUTHOR: Liodakis, I., Hovatta, T., Aller, M. F., Aller, H. D., Gurwell, M. A., Lähteenmäki, A., Tornikoski, M.
PUBLICATION: *Astronomy and Astrophysics, 654, A169*
PUBLICATION DATE: 10/2021
ABSTRACT: https://ui.adsabs.harvard.edu/abs/2021A&A...654A.169L
DOI: 10.1051/0004-6361/202141053

TITLE: Orientation effect on the light-curve shape of periodic methanol maser sources
AUTHOR: Morgan, J., van der Walt, D. J., Chibueze, J. O., Zhang, Q.
PUBLICATION: *Monthly Notices of the Royal Astronomical Society, 507, 1138-1148*
PUBLICATION DATE: 10/2021
ABSTRACT: https://ui.adsabs.harvard.edu/abs/2021MNRAS.507.1138M
DOI: 10.1093/mnras/stab2185

TITLE: Linking High- and Low-Mass Star Formation: Observation-Based Continuum Modelling and Physical Conditions
AUTHOR: Pitts, R. L., Kristensen, L. E., Jørgensen, J. K., van der Walt, S. J.
PUBLICATION: *arXiv e-prints, arXiv:2110.11132*
PUBLICATION DATE: 10/2021
ABSTRACT: https://ui.adsabs.harvard.edu/abs/2021arXiv211011132P

TITLE: Luminous Millimeter, Radio, and X-ray Emission from ZTF20acigmel (AT2020xnd)
AUTHOR: Ho, A. Y. Q., Margalit, B., Bremer, M., Perley, D. A., Yao, Y., Dobie, D., Kaplan, D. L., OBrien, A., Petitpas, G., Zic, A.
PUBLICATION: *arXiv e-prints, arXiv:2110.05490*
PUBLICATION DATE: 10/2021
ABSTRACT: https://ui.adsabs.harvard.edu/abs/2021arXiv211005490H

TITLE: Core Mass Function of a Single Giant Molecular Cloud Complex with 10,000 Cores
AUTHOR: Cao, Y., Qiu, K., Zhang, Q., Wang, Y., Xiao, Y.
PUBLICATION: *The Astrophysical Journal, 918, L4*
PUBLICATION DATE: 09/2021
ABSTRACT: https://ui.adsabs.harvard.edu/abs/2021ApJ...918L...4C
DOI: 10.3847/2041-8213/ac1947

TITLE: Discovery of a Highly Collimated Flow from the High-Mass Protostar ISOSS J23053+5953 SMM2
AUTHOR: M., T., Rodríguez, Hofner, P., Araya, E. D., Zhang, Q., Linz, H., Kurtz, S., Gómez, L., Carrasco-González, C., Rosero, V.
PUBLICATION: *arXiv e-prints, arXiv:2109.01243*
PUBLICATION DATE: 09/2021
ABSTRACT: https://ui.adsabs.harvard.edu/abs/2021arXiv210901243M

TITLE: Massive molecular gas reservoir in a luminous sub-millimeter galaxy during cosmic noon
AUTHOR: Liu, B., Chartab, N., Nayyeri, H., Cooray, A., Yang, C., Riechers, D. A., Gurwell, M., Zhu, Z.-. hong ., Serjeant, S., Borsato, E., Negrello, M., Marchetti, L., Corsini, E. M., van der Werf, P.
PUBLICATION: *arXiv e-prints, arXiv:2108.13016*
PUBLICATION DATE: 08/2021
ABSTRACT: https://ui.adsabs.harvard.edu/abs/2021arXiv210813016L

TITLE: Rapid Variability of Sgr A* across the Electromagnetic Spectrum
AUTHOR: Witzel, G., Martinez, G., Willner, S. P., Becklin, E. E., Boyce, H., Do, T., Eckart, A., Fazio, G. G., Ghez, A., Gurwell, M. A., Haggard, D., Herrero-Illana, R., Hora, J. L., Li, Z., Liu, J., Marchili, N., Morris, M. R., Smith, H. A., Subroweit, M., Zensus, J. A.
PUBLICATION: *The Astrophysical Journal, 917, 73*
PUBLICATION DATE: 08/2021
ABSTRACT: https://ui.adsabs.harvard.edu/abs/2021ApJ...917...73W
DOI: 10.3847/1538-4357/ac0891

TITLE: Event Horizon Telescope observations of the jet launching and collimation in Centaurus A
AUTHOR: Janssen, M., Falcke, H., Kadler, M., Ros, E., Wielgus, M., Akiyama, K., Baloković, M., Blackburn, L., Bouman, K. L., Chael, A., Chan, C.-. kwan ., Chatterjee, K., Davelaar, J., Edwards, P. G., Fromm, C. M., Gómez, J. L., Goddi, C., Issaoun, S., Johnson, M. D., Kim, J., Koay, J. Y., Krichbaum, T. P., Liu, J., Liuzzo, E., Markoff, S., Markowitz, A., Marrone, D. P., Mizuno, Y., Müller, C., Ni, C., Pesce, D. W., Ramakrishnan, V., Roelofs, F., Rygl, K. L. J., van Bemmel, I., Event Horizon Telescope Collaboration, Alberdi, A., Alef, W., Algaba, J. C., Anantua, R., Asada, K., Azulay, R., Baczko, A.-K., Ball, D., Ball, D., Barrett, J., Benson, B. A., Bintley, D., Bintley, D., Blundell, R., Boland, W., Boland, W., Bower, G. C., Boyce, H., Bremer, M., Brinkerink, C. D., Brissenden, R., Britzen, S., Broderick, A. E., Broguiere, D., Bronzwaer, T., Byun, D.-Y., Carlstrom, J. E., Chatterjee, S., Chen, M.-T., Chen, Y., Chesler, P. M., Cho, I., Christian, P., Conway, J. E., Cordes, J. M., Crawford, T. M., Crew, G. B., Cruz-Osorio, A., Cui, Y., Cui, Y., De Laurentis, M., Deane, R., Dempsey, J., Desvignes, G., Dexter, J., Doeleman, S. S., Eatough, R. P., Farah, J., Farah, J., Fish, V. L., Fomalont, E., Ford, H. A., Fraga-Encinas, R., Friberg, P., Friberg, P., Fuentes, A., Galison, P., Gammie, C. F., García, R., Gelles, Z., Gentaz, O., Georgiev, B., Georgiev, B., Gold, R., Gold, R., Gómez-Ruiz, A. I., Gu, M., Gurwell, M., Hada, K., Haggard, D., Hecht, M. H., Hesper, R., Himwich, E., Ho, L. C., Ho, P., Honma, M., Huang, C.-W. L., Huang, L., Hughes, D. H., Ikeda, S., Inoue, M., Inoue, M., James, D. J., Jannuzi, B. T., Jannuzi, B. T., Jeter, B., Jiang, W., Jimenez-Rosales, A., Jimenez-Rosales, A., Jorstad, S., Jung, T., Karami, M., Karuppusamy, R., Kawashima, T., Keating, G. K., Kettenis, M., Kim, D.-J., Kim, J.-Y., Kim, J.-Y., Kim, J., Kino, M., Kino, M., Kofuji, Y., Koyama, S., Kramer, M., Kramer, C., Kramer, C., Kuo, C.-Y., Lauer, T. R., Lee, S.-S., Levis, A., Li, Y.-R., Li, Z., Lindqvist, M., Lico, R., Lindahl, G., Lindahl, G., Liu, K., Liu, K., Lo, W.-P., Lobanov, A. P., Loinard, L., Lonsdale, C., Lu, R.-S., MacDonald, N. R., Mao, J., Marchili, N., Marchili, N., Marchili, N., Marscher, A. P., Martí-Vidal, I., Matsushita, S., Matthews, L. D., Medeiros, L., Menten, K. M., Mizuno, I., Mizuno, I., Moran, J. M., Moriyama, K., Moscibrodzka, M., Moscibrodzka, M., Musoke, G., Mejías, A. M., Nagai, H., Nagar, N. M., Nakamura, M., Narayan, R., Narayanan, G., Natarajan, I., Nathanail, A., Neilsen, J., Neri, R., Neri, R., Noutsos, A., Nowak, M. A., Okino, H., Olivares, H., Ortiz-León, G.

N., Oyama, T., Özel, F., Palumbo, D. C. M., Park, J., Patel, N., Pen, U.-L., Pen, U.-L., Piétu, V., Plambeck, R., PopStefanija, A., Porth, O., Pötzl, F. M., Prather, B., Preciado-López, J. A., Psaltis, D., Pu, H.-Y., Pu, H.-Y., Rao, R., Rawlings, M. G., Raymond, A. W., Rezzolla, L., Ricarte, A., Ripperda, B., Ripperda, B., Rogers, A., Rogers, A., Rose, M., Roshanineshat, A., Rottmann, H., Roy, A. L., Ruszczyk, C., Ruszczyk, C., Sánchez, S., Sánchez-Arguelles, D., Sasada, M., Savolainen, T., Schloerb, F. P., Schuster, K.-F., Shao, L., Shen, Z., Small, D., Sohn, B. W., SooHoo, J., Sun, H., Tazaki, F., Tetarenko, A. J., Tiede, P., Tilanus, R. P. J., Titus, M., Torne, P., Trent, T., Traianou, E., Trippe, S., van Bemmel, I., van Langevelde, H. J., van Rossum, D. R., Wagner, J., Ward-Thompson, D., Wardle, J., Weintroub, J., Wex, N., Wharton, R., Wharton, R., Wong, G. N., Wu, Q., Yoon, D., Young, A., Young, K., Younsi, Z., Yuan, F., Yuan, Y.-F., Zensus, J. A., Zhao, G.-Y., Zhao, S.-S.

PUBLICATION: *Nature Astronomy, 5, 1017-1028*

PUBLICATION DATE: 07/2021

ABSTRACT: https://ui.adsabs.harvard.edu/abs/2021NatAs...5.1017J

DOI: 10.1038/s41550-021-01417-w

TITLE: The Polarized Image of a Synchrotron-emitting Ring of Gas Orbiting a Black Hole

AUTHOR: Narayan, R., Palumbo, D. C. M., Johnson, M. D., Gelles, Z., Himwich, E., Chang, D. O., Ricarte, A., Dexter, J., Gammie, C. F., Chael, A. A., Event Horizon Telescope Collaboration, Akiyama, K., Alberdi, A., Alef, W., Algaba, J. C., Anantua, R., Asada, K., Azulay, R., Baczko, A.-K., Ball, D., Baloković, M., Barrett, J., Benson, B. A., Bintley, D., Blackburn, L., Blundell, R., Boland, W., Bouman, K. L., Bower, G. C., Boyce, H., Bremer, M., Brinkerink, C. D., Brissenden, R., Britzen, S., Broderick, A. E., Broguiere, D., Bronzwaer, T., Byun, D.-Y., Carlstrom, J. E., Chan, C.-. kwan ., Chatterjee, S., Chatterjee, K., Chen, M.-T., Chen, Y., Chesler, P. M., Cho, I., Christian, P., Conway, J. E., Cordes, J. M., Crawford, T. M., Crew, G. B., Cruz-Osorio, A., Cui, Y., Davelaar, J., De Laurentis, M., Deane, R., Dempsey, J., Desvignes, G., Doeleman, S. S., Eatough, R. P., Falcke, H., Farah, J., Fish, V. L., Fomalont, E., Ford, H. A., Fraga-Encinas, R., Friberg, P., Fromm, C. M., Fuentes, A., Galison, P., García, R., Gentaz, O., Georgiev, B., Goddi, C., Gold, R., Gómez, J. L., Gómez-Ruiz, A. I., Gu, M., Gurwell, M., Hada, K., Haggard, D., Hecht, M. H., Hesper, R., Ho, L. C., Ho, P., Honma, M., Huang, C.-W. L., Huang, L., Hughes, D. H., Ikeda, S., Inoue, M., Issaoun, S., James, D. J., Jannuzi, B. T., Janssen, M., Jeter, B., Jiang, W., Jimenez-Rosales, A., Jorstad, S., Jung, T., Karami, M., Karuppusamy, R., Kawashima, T., Keating, G. K., Kettenis, M., Kim, D.-J., Kim, J.-Y., Kim, J., Kim, J., Kino, M., Koay, J. Y., Kofuji, Y., Koch, P. M., Koyama, S., Kramer, M., Kramer, C., Krichbaum, T. P., Kuo, C.-Y., Lauer, T. R., Lee, S.-S., Levis, A., Li, Y.-R., Li, Z., Lindqvist, M., Lico, R., Lindahl, G., Liu, J., Liu, K., Liuzzo, E., Lo, W.-P., Lobanov, A. P., Loinard, L., Lonsdale, C., Lu, R.-S., MacDonald, N. R., Mao, J., Marchili, N., Markoff, S., Marrone, D. P., Marscher, A. P., Martí-Vidal, I., Matsushita, S., Matthews, L. D., Medeiros, L., Menten, K. M., Mizuno, I., Mizuno, Y., Moran, J. M., Moriyama, K., Moscibrodzka, M., Müller, C., Musoke, G., Mejías, A. M., Nagai, H., Nagar, N. M., Nakamura, M., Narayanan, G., Natarajan, I., Nathanail, A., Neilsen, J., Neri, R., Ni, C., Noutsos, A., Nowak, M. A., Okino, H., Olivares, H., Ortiz-León, G. N., Oyama, T., Özel, F., Park, J., Patel, N., Pen, U.-L., Pesce, D. W., Piétu, V., Plambeck, R., PopStefanija, A., Porth, O., Pötzl, F. M., Prather, B., Preciado-López, J. A., Psaltis, D., Pu, H.-Y., Ramakrishnan, V., Rao, R., Rawlings, M. G., Raymond, A. W., Rezzolla, L., Ripperda, B., Roelofs, F., Rogers, A., Ros, E., Rose, M., Roshanineshat, A., Rottmann, H., Roy, A. L., Ruszczyk, C., Rygl, K. L. J., Sánchez, S., Sánchez-Arguelles, D., Sasada, M., Savolainen, T., Schloerb, F. P., Schuster, K.-F., Shao, L., Shen, Z., Small, D., Sohn, B. W., SooHoo, J., Sun, H., Tazaki, F., Tetarenko, A. J., Tiede, P., Tilanus, R. P. J., Titus, M., Toma, K., Torne, P., Trent, T., Traianou, E., Trippe, S., van Bemmel, I., van Langevelde, H. J., van Rossum, D. R., Wagner, J., Ward-Thompson, D., Wardle, J., Weintroub, J., Wex, N., Wharton, R., Wielgus, M., Wong, G. N., Wu, Q., Yoon, D., Young, A., Young, K., Younsi, Z., Yuan, F., Yuan, Y.-F., Zensus, J. A., Zhao, G.-Y., Zhao, S.-S.

PUBLICATION: *The Astrophysical Journal, 912, 35*

PUBLICATION DATE: 05/2021

ABSTRACT: https://ui.adsabs.harvard.edu/abs/2021ApJ...912...35N

DOI: 10.3847/1538-4357/abf117

TITLE: Does the Magnetic Field Suppress Fragmentation in Massive Dense Cores?
AUTHOR: Palau, A., Zhang, Q., Girart, J. M., Liu, J., Rao, R., Koch, P. M., Estalella, R., Chen, H.-R. V., Liu, H. B., Qiu, K., Li, Z.-Y., Zapata, L. A., Bontemps, S., Ho, P. T. P., Beuther, H., Ching, T.-C., Shinnaga, H., Ahmadi, A.
PUBLICATION: *The Astrophysical Journal, 912, 159*
PUBLICATION DATE: 05/2021
ABSTRACT: https://ui.adsabs.harvard.edu/abs/2021ApJ...912..159P
DOI: 10.3847/1538-4357/abee1e

TITLE: Constraints on the Mass Accretion Rate onto the Supermassive Black Hole of Cygnus A Using the Submillimeter Array
AUTHOR: Lo, W.-P., Asada, K., Matsushita, S., Nakamura, M., Pu, H.-Y., Tseng, C., Akiyama, K., Algaba, J. C., Bower, G. C., Rao, R., Koay, J. Y., Koch, P. M., Koyama, S., Ho, P. T. P., Inoue, M.
PUBLICATION: *The Astrophysical Journal, 911, 35*
PUBLICATION DATE: 04/2021
ABSTRACT: https://ui.adsabs.harvard.edu/abs/2021ApJ...911...35L
DOI: 10.3847/1538-4357/abd17b

The Submillimeter Array (SMA) is a pioneering radio-interferometer dedicated to a broad range of astronomical studies including finding protostellar disks and outflows; evolved stars; the Galactic Center and AGN; normal and luminous galaxies; and the solar system. Located on Maunakea, Hawaii, the SMA is a collaboration between the Smithsonian Astrophysical Observatory and the Academia Sinica Institute of Astronomy and Astrophysics.

SUBMILLIMETER ARRAY
Center for Astrophysics | Harvard & Smithsonian
60 Garden Street, MS 78
Cambridge, MA 02138 USA
www.cfa.harvard.edu/sma/

SMA HILO OFFICE
645 North A'ohoku Place
Hilo, Hawaii 96720
Ph. 808.961.2920
Fx. 808.961.2921
sma1.sma.hawaii.edu

ACADEMIA SINICA INSTITUTE
OF ASTRONOMY & ASTROPHYSICS
11F of Astronomy-Mathematics Building,
AS/NTU, No. 1, Sec. 4, Roosevelt Road
Taipei 10617
Taiwan R.O.C.
www.asiaa.sinica.edu.tw/